Baryogenesis in R^2-Higgs inflation: The gravitational connection

Yann Cado[,1] Christoph Englert[,2] Tanmoy Modak[,3] and Mariano Quirós[4]

[1]*Laboratoire de Physique Théorique et Hautes Energies (LPTHE),*
Sorbonne Université et CNRS UMR 7589, 4 place Jussieu, 75252 Paris CEDEX 05, France
[2]*School of Physics & Astronomy, University of Glasgow, Glasgow G12 8QQ, United Kingdom*
[3]*Institut für Theoretische Physik, Universität Heidelberg, 69120 Heidelberg, Germany*
[4]*Institut de Física d'Altes Energies (IFAE) and The Barcelona Institute of Science and Technology (BIST),*
Campus UAB, 08193 Bellaterra, Barcelona, Spain

R^2-Higgs inflation stands out as one of the best-fit models of Planck data. Using a covariant formalism for the inflationary dynamics and the production of helical gauge fields, we show that the observed baryon asymmetry of the Universe (BAU) can be obtained when this model is supplemented by a dimension-six CP-violating term $\sim (R/\Lambda^2) B_{\mu\nu} \tilde{B}^{\mu\nu}$ in the hypercharge sector. At linear order, values of $\Lambda \simeq 2.5 \times 10^{-5} M_{\rm P}$ produce, in the R^2-like regime, sufficient helical hypermagnetic fields to create the observed matter-antimatter asymmetry during the electroweak crossover. However, the Schwinger effect of fermion pair production can play a critical role in this context, and that scale is significantly lowered when the backreaction of the fermion fields on the gauge field production is included. In all cases, the helical field configurations can remain robust against washout after the end of inflation.

I. INTRODUCTION

Cosmic inflation [1–3] elegantly addresses a plethora of observations, ranging from the flatness of the Universe, over resolving the horizon and exotic relics problems, all the way to seeding the primordial density perturbations giving rise to the large-scale structure of the Universe that we see today. In parallel, it can explain the cosmic microwave background (CMB) anisotropies measured by experiments such as Planck [4]. While there are several alternatives to inflation, among these models, Starobinsky or R^2 [1,5–8] inflation, where pure general relativity (GR) is extended by an additional scalar curvature term R^2, is one of the best-fitting models of current data [4].

In the dual scalar-tensor theory, the presence of the R^2 term makes the scalar degree of freedom dynamical, which can account for cosmic inflation. After the discovery of the Higgs boson at the Large Hadron Collider (LHC) [9,10], the theory essentially contains two scalar degrees of freedom. Indeed, if the Higgs field Φ couples nonminimally to the Ricci scalar R via a term $\xi_H R |\Phi|^2$, with ξ_H as the nonminimal coupling, the Higgs field itself can induce inflation [11–17] (for earlier works which employed similar mechanisms, see Refs. [18–25]). In pure Higgs inflation, i.e., without the presence of such R^2 term, a scale of unitarity violation emerges [26–29]. This may not pose a threat to inflationary dynamics, see Ref. [30]. However, during the preheating stage, longitudinal gauge bosons with momenta beyond the unitarity cutoff scale are

violently produced [31–33]. The perturbative unitarity is restored up to the Planck scale due to the presence of R^2 term in R^2-Higgs inflation [34] (see also, e.g., [35–46]). Moreover, R^2-Higgs inflation (or the Starobinsky-Higgs inflation), which features both the R^2 and $R|\Phi|^2$ terms, is also the best-fit model for the Planck data.

Following on from these successes, it is not unreasonable to correlate the R^2-Higgs inflation to the other shortcomings of the current microscopic theory of interactions, the Standard Model of particle physics (SM). One such shortfall is the observed matter-antimatter asymmetry (or the baryon asymmetry) of the Universe, BAU. The existence of the BAU is a strong indicator of the presence of interactions beyond the SM. A range of particle physics experiments, chiefly at the LHC, are searching for such interactions at the currently largest available energy scales of $\mathcal{O}(\text{TeV})$. If the fundamental scale of the mechanism behind the BAU is tied to a higher scale, it might be possible that tell-tale effects at present or even future colliders could remain absent. In the SM, the CP-violation from the CKM matrix is not sufficient for baryogenesis [47–49]. Further, the electroweak phase transition in the SM is a continuous crossover [50] rather than the typically desired strong first-order transition to drive the departure from thermal equilibrium condition as part of Sakharov's criteria [51]. However, even at the crossover, the out-of-equilibrium condition can be met if the source and washout decay rates are different and shut off at different epochs [52,53]. If the inflaton field couples to the CP-odd hypercharge Chern-Simons density $F\tilde{F}$, with F

and $\tilde{F}$ denoting the field-stress tensor of a $U(1)$ gauge field (which mixes with the hypercharge gauge field) and its dual, respectively, helical hypermagnetic fields can be abundantly produced at the end of inflation [54–59]. The helical hypermagnetic fields may then create the observed baryon asymmetry at the electroweak crossover [53,60–65].

In this article, we investigate baryogenesis in R^2-Higgs inflation from CP-violating dimension-six Chern-Simons density $\sim (R/\Lambda^2) B_{\mu\nu} \tilde{B}^{\mu\nu}$, where R is the Ricci scalar and $B_{\mu\nu}$ is the field stress tensor of $U(1)_Y$ hypercharge in the Jordan frame (see also Refs. [66–70] for similar discussions). This term can be considered within the context extended theories of gravity (or rather, $f(R, \phi, B_\mu)$ gravity), and it elegantly connects high-scale BAU to inflationary dynamics without requiring additional fields beyond the SM. Adopting the covariant formalism due to the noncanonical kinetic terms in R^2-Higgs inflation, our linear order analysis, with $\Lambda \sim 10^{-5} M_P$, demonstrates that the produced helical hypermagnetic fields are sufficient to account for the BAU. We take into account effects that could lead to a washout of the helicity stored in the gauge sector (e.g., the chiral plasma instability) alongside observational bounds on a range of associated phenomena that prevent total freedom of the possible field configurations.

In the presence of strong gauge fields, light fermions charged under the gauge group are produced by the backreaction of gauge fields that source the fermions equation of motion [71,72]. The corresponding currents can then, in turn, backreact on the produced gauge fields, a phenomenon called the *Schwinger effect*, see e.g. Ref. [73]. The backreaction of fermion currents on the produced gauge fields acts as a damping force during the explosive production of helical gauge fields, and many of the conclusions from the gauge field production should be revised in the presence of the Schwinger effect. In particular, it has been shown that, although the amount of gauge energy density is suppressed, which jeopardizes the gauge preheating capabilities, there is still a window for the baryogenesis mechanism, see Ref. [65]. Also, one possible way out is if there are no light, charged fermion fields when gauge fields are produced, for instance by the use of a special Froggatt-Nielsen mechanism such that all fermion Yukawa couplings stay large at the end of inflation, while they relax after inflation to the measured values [74]. However, in this paper, we will stay agnostic on the fermions effect in the plasma and provide the results with and without the Schwinger effect.

We organize this paper as follows. We start with outlining the action and derive the relevant equations of motion (EoM) for different fields in Sec. II, followed by the inflationary dynamics in the covariant formalism in Sec. III. The production of hypermagnetic fields and subsequent generation of the BAU are discussed, respectively, in Secs. IV and V. We summarize with some discussion in Sec. VI. Finally, we present some technical computational details through appendices A–E.

II. THE STAROBINSKY-HIGGS ACTION

In pure GR with a canonically coupled scalar theory, without the presence of R^2, the conformal mode of the metric is known to have a wrong-sign kinetic term. The Starobinsky inflation model, which extends pure GR with an additional scalar curvature term R^2, falls within the so-called general $f(R)$ theory of gravity. In its dual scalar-tensor theory, the presence of the R^2 term makes the scalar degree of freedom dynamical, which can then account for cosmic inflation. R^2-Higgs inflation (or Starobinsky-Higgs inflation), which features all possible dimension-four terms i.e., both the R^2 and $R|\Phi|^2$ terms also provide best-fit models of the Planck data. The model has two dynamical scalar degrees of freedom, one appearing from the gravity sector and one entering as part of the Higgs field Φ.

We briefly discuss the action and its transformation properties in the metric formalism assuming the affine connection to be the Levi-Civita connection. The action in the Jordan frame of R^2-Higgs inflation, along with a dimension-six CP-odd term coupling Ricci scalar and $U(1)_Y$ gauge boson, is given by

$$S_J = \int d^4x \sqrt{-g_J} \left[\frac{M_P^2}{2} f(R_J, \Phi, B_\mu) \right.$$
$$- g_J^{\mu\nu} (\nabla_\mu \Phi)^\dagger \nabla_\nu \Phi - V(\Phi, \Phi^\dagger) - \frac{1}{4} g_J^{\mu\rho} g_J^{\nu\sigma} B_{\mu\nu} B_{\rho\sigma}$$
$$\left. - \frac{1}{4} g_J^{\mu\rho} g_J^{\nu\sigma} W_{\mu\nu}^i W_{\rho\sigma}^i - \sum_f g_J^{\mu\nu} \bar{f} e_\mu^a \tilde{\gamma}_a \nabla_\nu^f f \right], \quad (2.1)$$

and we adopt a mostly-plus convention for the metric $(-1, +1, +1, +1)$. From here on, for notational simplicity, we will remove the sum over fermions $\sum_f$ in the fermion quadratic terms, which will remain implicit. The $B_{\mu\nu}$ and $W_{\mu\nu}^i$ are field stress tensors of the $U(1)_Y$ and $SU(2)_L$ gauge groups, respectively, Φ is the Higgs field, R_J the Ricci scalar in the Jordan frame, and $M_P = \sqrt{1/(8\pi G)} = 2.435 \times 10^{18}$ GeV, where G is the Newton's constant and M_P the reduced Planck mass. We use the convention $\epsilon^{0123} = 1$ for the Levi-Civita tensor. The covariant derivatives are defined as

$$\nabla_\mu = D_\mu + ig' \frac{1}{2} Q_{Y_f} B_\mu + ig \frac{1}{2} \boldsymbol{\tau} \cdot \boldsymbol{W}_\mu, \quad (2.2a)$$

$$\nabla_\mu^f f = \left(D_\mu^f + ig' \frac{1}{2} Q_{Y_f} B_\mu + ig \frac{1}{2} \boldsymbol{\tau} \cdot \boldsymbol{W}_\mu \right) f, \quad (2.2b)$$

with Q_{Y_f} denoting the $U(1)_Y$ hypercharge, $\boldsymbol{\tau}$ are the Pauli matrices, and g' and g are respective gauge couplings. D_μ is the usual covariant derivative with respect to the space-time

metric $g_{J\mu\nu}$ and $D_\mu^f \equiv \partial_\mu + \Gamma_\mu$ is the covariant derivative of spinors, with Γ_μ as the spin affine connection. Here e_μ^a is the so-called vierbein and $\tilde{\gamma}_a$ is Minkowski space gamma matrices (see Appendix A for details of the formalism and the definition of Γ_μ). The corresponding field-stress tensors for the $U(1)_Y$ and $SU(2)_L$ gauge fields are

$$B_{\mu\nu} = D_\mu B_\nu - D_\nu B_\mu, \qquad W_{\mu\nu}^i = D_\mu W_\nu^i - D_\nu W_\mu^i - g \sum_{j,k=1}^3 \epsilon_{ijk} W_\mu^j W_\nu^k. \tag{2.3}$$

The Higgs potential $V(\Phi, \Phi^\dagger)$ and $f(R_J, \Phi, B_\mu)$ are given as[1]

$$V(\Phi, \Phi^\dagger) = \lambda |\Phi|^4, \tag{2.4a}$$

$$f(R_J, \Phi, B_\mu) = R_J + \frac{\xi_R}{2M_P^2} R_J^2 + \frac{2\xi_H}{M_P^2} |\Phi|^2 R_J - \frac{2}{\Lambda^2 M_P^2} \frac{\epsilon^{\mu\nu\rho\sigma}}{\sqrt{-g_J}} B_{\mu\nu} B_{\rho\sigma} R_J. \tag{2.4b}$$

The Higgs field has hypercharge $+1$ and is decomposed in the standard way (we will comment on our gauge choice further below)

$$\Phi = \frac{1}{\sqrt{2}} \begin{pmatrix} 0 \\ h \end{pmatrix}. \tag{2.5}$$

With this choice, Eq. (2.1) becomes

$$\begin{aligned} S_J = \int d^4x \sqrt{-g_J} &\left[\frac{M_P^2}{2} f(R_J, h, B_\mu) - \frac{1}{2} g_J^{\mu\nu} (D_\mu h) D_\nu h - V(h) \right. \\ &- \frac{1}{4} g_J^{\mu\nu} g^2 h^2 \frac{(W_\mu^1 - iW_\mu^2)}{\sqrt{2}} \frac{(W_\nu^1 + iW_\nu^2)}{\sqrt{2}} - \frac{1}{8} g_J^{\mu\nu} h^2 (gW_\mu^3 - g'B_\mu)(gW_\nu^3 - g'B_\nu) \\ &\left. - \frac{1}{4} g_J^{\mu\rho} g_J^{\nu\sigma} B_{\mu\nu} B_{\rho\sigma} - \frac{1}{4} g_J^{\mu\rho} g_J^{\nu\sigma} W_{\mu\nu}^i W_{\rho\sigma}^i - g_J^{\mu\nu} \bar{f} e_\mu^a \tilde{\gamma}_a \nabla_\nu^f f \right], \end{aligned} \tag{2.6}$$

with

$$V(h) = \frac{\lambda}{4} h^4, \qquad f(R_J, h, B_\mu) = R_J + \frac{\xi_R}{2M_P^2} R_J^2 + \frac{\xi_H}{M_P^2} h^2 R_J - \frac{2}{\Lambda^2 M_P^2} \frac{\epsilon^{\mu\nu\rho\sigma}}{\sqrt{-g_J}} B_{\mu\nu} B_{\rho\sigma} R_J. \tag{2.7}$$

The dynamics of the scalar degrees of freedom are easily captured once we move from the Jordan frame to the Einstein frame via a Weyl transformation. We first introduce an auxiliary field Ψ and rewrite the action in Eq. (2.6) as

$$\begin{aligned} S_J = \int d^4x \sqrt{-g_J} &\left[\frac{M_P^2}{2} \left(f(\Psi, h, B_\mu) + \frac{\partial f(\Psi, h, B_\mu)}{\partial \Psi} (R_J - \Psi) \right) - \frac{1}{2} g_J^{\mu\nu} (D_\mu h)(D_\nu h) - V(h) \right. \\ &- \frac{1}{4} g_J^{\mu\nu} g^2 h^2 \frac{(W_\mu^1 - iW_\mu^2)}{\sqrt{2}} \frac{(W_\nu^1 + iW_\nu^2)}{\sqrt{2}} - \frac{1}{8} g_J^{\mu\nu} h^2 (gW_\mu^3 - g'B_\mu)(gW_\nu^3 - g'B_\nu) \\ &\left. - \frac{1}{4} g_J^{\mu\rho} g_J^{\nu\sigma} B_{\mu\nu} B_{\rho\sigma} - \frac{1}{4} g_J^{\mu\rho} g_J^{\nu\sigma} W_{\mu\nu}^i W_{\rho\sigma}^i - g_J^{\mu\nu} \bar{f} e_\mu^a \tilde{\gamma}_a \nabla_\nu^f f \right]. \end{aligned} \tag{2.8}$$

The variation with respect to Ψ gives the constraint $\Psi = R_J$ as long as $\partial^2 f(\Psi, h, B_\mu)/\partial\Psi^2 \neq 0$. We now define a physical degree of freedom Θ as

---

[1] For large configuration values of the Higgs field we can consistently neglect the mass term of the Higgs potential, which triggers electroweak symmetry breaking.

$$\Theta = \frac{\partial f(\Psi, h, B_\mu)}{\partial \Psi} \tag{2.9}$$

such that the action Eq. (2.8) can be cast into

$$
\begin{aligned}
S_J = \int d^4x \sqrt{-g_J} \Bigg[&\frac{M_P^2}{2} \Theta R_J - U(\Theta, h, B_\mu) - \frac{1}{2} g_J^{\mu\nu} (D_\mu h)(D_\nu h) - V(h) - \frac{1}{4} g_J^{\mu\rho} g_J^{\nu\sigma} B_{\mu\nu} B_{\rho\sigma} \\
&- \frac{1}{4} g_J^{\mu\nu} g^2 h^2 \frac{(W_\mu^1 - iW_\mu^2)}{\sqrt{2}} \frac{(W_\nu^1 + iW_\nu^2)}{\sqrt{2}} - \frac{1}{8} g_J^{\mu\nu} h^2 (gW_\mu^3 - g'B_\mu)(gW_\nu^3 - g'B_\nu) \\
&- \frac{1}{4} g_J^{\mu\rho} g_J^{\nu\sigma} W_{\mu\nu}^i W_{\rho\sigma}^i - g_J^{\mu\nu} \bar{f} e_\mu^a \tilde{\gamma}_a \nabla_\nu^f f \Bigg],
\end{aligned}
\tag{2.10}
$$

with the definition

$$
\begin{aligned}
U(\Theta, h, B_\mu) &= \frac{M_P^2}{2} [\Psi(\Theta)\Theta - f(\Psi(\Theta), h, B_\mu)] \\
&= \frac{M_P^4}{4\xi_R} \left(1 - \Theta + \frac{\xi_H}{M_P^2} h^2 - \frac{2}{\Lambda^2 M_P^2} \frac{\epsilon^{\mu\nu\rho\sigma}}{\sqrt{-g_J}} B_{\mu\nu} B_{\rho\sigma} \right)^2.
\end{aligned}
\tag{2.11}
$$

To formulate the action in the Einstein frame, we perform the metric redefinition (Weyl transformation)

$$g_{J\mu\nu} = \frac{1}{\Theta} g_{E\mu\nu}, \qquad g_J^{\mu\nu} = \Theta g_E^{\mu\nu}, \quad \text{and} \quad \sqrt{-g_J} = \frac{1}{\Theta^2} \sqrt{-g_E}. \tag{2.12}$$

Under this transformation, the Ricci scalar transforms as

$$R_J = \Theta \left[R_E + 3\Box_E \Theta - \frac{3}{2} g_E^{\mu\nu} D_\mu(\ln\Theta) D_\nu(\ln\Theta) \right], \tag{2.13}$$

with $\Box_E = g_E^{\mu\nu} D_\mu D_\nu$. Ignoring the surface term, the action of Eq. (2.8) now becomes

$$
\begin{aligned}
S_E = \int d^4x \sqrt{-g_E} \Bigg[&\frac{M_P^2}{2} R_E - \frac{3M_P^2}{4} g_E^{\mu\nu} D_\mu(\ln\Theta) D_\nu(\ln\Theta) - \frac{1}{2\Theta} g_E^{\mu\nu} (D_\mu h)(D_\nu h) - V_E \\
&- \frac{1}{4} g_E^{\mu\rho} g_E^{\nu\sigma} B_{\mu\nu} B_{\rho\sigma} - \frac{1}{4\Theta} g_E^{\mu\nu} g^2 h^2 \frac{(W_\mu^1 - iW_\mu^2)}{\sqrt{2}} \frac{(W_\nu^1 + iW_\nu^2)}{\sqrt{2}} \\
&- \frac{1}{8\Theta} g_E^{\mu\nu} h^2 (gW_\mu^3 - g'B_\mu)(gW_\nu^3 - g'B_\nu) - \frac{1}{4} g_E^{\mu\rho} g_E^{\nu\sigma} W_{\mu\nu}^i W_{\rho\sigma}^i - \frac{1}{\Theta} g_E^{\mu\nu} \bar{f} e_\mu^a \tilde{\gamma}_a \nabla_\nu^f f \Bigg],
\end{aligned}
\tag{2.14}
$$

with

$$V_E = \frac{1}{\Theta^2} [V(h) + U(\Theta, h, B_\mu)]. \tag{2.15}$$

Finally, we perform the field redefinition

$$\phi = M_P \sqrt{\frac{3}{2}} \ln\Theta. \tag{2.16}$$

to arrive at the action in the form

$$S_E = \int d^4x \sqrt{-g_E} \left[\frac{M_P^2}{2} R_E - \frac{1}{2} G_{IJ} g_E^{\mu\nu} D_\mu \phi^I D_\nu \phi^J - V_E(\phi^I) - \frac{1}{4} g_E^{\mu\rho} g_E^{\nu\sigma} B_{\mu\nu} B_{\rho\sigma} \right.$$
$$- \frac{1}{4} g_E^{\mu\rho} g_E^{\nu\sigma} W_{\mu\nu}^i W_{\rho\sigma}^i - \frac{1}{4} e^{-\sqrt{\frac{2}{3}}\frac{\phi}{M_P}} g_E^{\mu\nu} g^2 h^2 \frac{(W_\mu^1 - iW_\mu^2)}{\sqrt{2}} \frac{(W_\nu^1 + iW_\nu^2)}{\sqrt{2}}$$
$$\left. - \frac{1}{8} e^{-\sqrt{\frac{2}{3}}\frac{\phi}{M_P}} g_E^{\mu\nu} h^2 (gW_\mu^3 - g'B_\mu)(gW_\nu^3 - g'B_\nu) - e^{-\sqrt{\frac{2}{3}}\frac{\phi}{M_P}} g_E^{\mu\nu} \bar{f} e_\mu^a \tilde{\gamma}_a \nabla_\nu^f f \right]. \tag{2.17}$$

The multi-field $\phi^I \in \{\phi, h\}$ alongside the field-space metric G_{IJ}

$$G_{\phi\phi} = 1, \qquad G_{\phi h} = G_{h\phi} = 0, \qquad G_{hh} = e^{-\sqrt{\frac{2}{3}}\frac{\phi}{M_P}} \tag{2.18}$$

highlight that we are working with a noncanonical kinetic term as alluded to above (see Appendix B for the corresponding field-space Christoffel symbols). The potential $V_E(\phi^I)$, consistently truncated at dimension-six level, reads

$$V_E(\phi^I) = e^{-2\sqrt{\frac{2}{3}}\frac{\phi}{M_P}} \left[\frac{\lambda}{4} h^4 + \frac{M_P^4}{4\xi_R} \left(1 - e^{\sqrt{\frac{2}{3}}\frac{\phi}{M_P}} + \frac{\xi_H}{M_P^2} h^2 - \frac{2}{\Lambda^2 M_P^2} \frac{\epsilon^{\mu\nu\rho\sigma}}{\sqrt{-g_E}} e^{2\sqrt{\frac{2}{3}}\frac{\phi}{M_P}} B_{\mu\nu} B_{\rho\sigma} \right)^2 \right]$$
$$= V_0(\phi^I) + \frac{2M_P^2}{\xi_R \Lambda^2} F(\phi^I) e^{\sqrt{\frac{2}{3}}\frac{\phi}{M_P}} B_{\mu\nu} \tilde{B}^{\mu\nu}, \tag{2.19}$$

with

$$V_0(\phi^I) = \frac{\lambda}{4} h^4 e^{-2\sqrt{\frac{2}{3}}\frac{\phi}{M_P}} + \frac{M_P^4}{4\xi_R} F^2(\phi^I), \tag{2.20a}$$

$$F(\phi^I) = 1 - e^{-\sqrt{\frac{2}{3}}\frac{\phi}{M_P}} + \frac{\xi_H}{M_P^2} h^2 e^{-\sqrt{\frac{2}{3}}\frac{\phi}{M_P}}, \qquad \tilde{B}^{\mu\nu} = \frac{1}{2\sqrt{-g_E}} \epsilon^{\mu\nu\rho\sigma} B_{\rho\sigma}. \tag{2.20b}$$

Note that the unmodified Starobinsky potential is recovered when the $B_{\mu\nu}\tilde{B}^{\mu\nu}$ term is absent.

We can now turn to the EoMs of the different fields in Eq. (2.17). By varying Eq. (2.17) with respect to the field ϕ, we obtain

$$\Box \phi^K + \Gamma_{IJ}^K g_E^{\alpha\nu} D_\alpha \phi^I D_\nu \phi^J - G^{KM} V_{E,M} + g_E^{\mu\nu} \mathcal{X}_{\mu\nu}^K = 0, \tag{2.21}$$

identifying Γ_{IJ}^K as the field-space Christoffel symbols and

$$\mathcal{X}_{\mu\nu}^K = \frac{1}{4} \sqrt{\frac{2}{3}} \frac{1}{M_P} G^{K1} e^{-\sqrt{\frac{2}{3}}\frac{\phi}{M_P}} g^2 h^2 \frac{(W_\mu^1 - iW_\mu^2)}{\sqrt{2}} \frac{(W_\nu^1 + iW_\nu^2)}{\sqrt{2}} - \frac{1}{2} e^{-\sqrt{\frac{2}{3}}\frac{\phi}{M_P}} G^{K2} g^2 h \frac{(W_\mu^1 - iW_\mu^2)}{\sqrt{2}} \frac{(W_\nu^1 + iW_\nu^2)}{\sqrt{2}}$$
$$+ \frac{1}{8} \sqrt{\frac{2}{3}} \frac{1}{M_P} G^{K1} e^{-\sqrt{\frac{2}{3}}\frac{\phi}{M_P}} h^2 (gW_\mu^3 - g'B_\mu)(gW_\nu^3 - g'B_\nu) - \frac{1}{4} G^{K2} e^{-\sqrt{\frac{2}{3}}\frac{\phi}{M_P}} h (gW_\mu^3 - g'B_\mu)(gW_\nu^3 - g'B_\nu)$$
$$+ \sqrt{\frac{2}{3}} \frac{1}{M_P} \delta_1^K e^{-\sqrt{\frac{2}{3}}\frac{\phi}{M_P}} g_E^{\mu\nu} \bar{f} t_\mu^a \tilde{\gamma}_a \nabla_\nu^f f. \tag{2.22}$$

Note that all the terms in $\mathcal{X}_{\mu\nu}^K$ are quadratic in the gauge fields.

The energy-momentum tensor $T_{\mu\nu}$ describes relevant quantities of the inflationary dynamics such as energy density or pressure. One can derive the Einstein-Hilbert equation from the action S_E by varying it with respect to $g_E^{\mu\nu}$

$$R_{E\mu\nu} - \frac{1}{2} g_{E\mu\nu} R_E = \frac{1}{M_P^2} \left(\mathcal{L}_M g_{E\mu\nu} - 2\frac{\delta(\mathcal{L}_M)}{\delta g_E^{\mu\nu}} \right) \tag{2.23}$$

and identify $T_{\mu\nu}$ as

$$T_{\mu\nu} = \left(\mathcal{L}_M g_{E\mu\nu} - 2 \frac{\delta(\mathcal{L}_M)}{\delta g_E^{\mu\nu}} \right). \tag{2.24}$$

Appendix C provides the full expression of $T_{\mu\nu}$ for the model considered in this work.

The EoM for the gauge field B_μ is given as

$$g_E^{\mu\alpha} g_E^{\nu\beta} D_\alpha B_{\mu\nu} + \frac{8M_P^2}{\xi_R \Lambda^2} D_\alpha (F(\phi^I) e^{\sqrt{\frac{2}{3}} \frac{\phi}{M_P}}) \tilde{B}^{\alpha\beta} + \left[\frac{g'}{4} e^{-\sqrt{\frac{2}{3}} \frac{\phi}{M_P}} g_E^{\mu\beta} h^2 (g W_\mu^3 - g' B_\mu) \right]$$

$$- \frac{ig' Q_{Y_f}}{2} e^{-\sqrt{\frac{2}{3}} \frac{\phi}{M_P}} g_E^{\mu\beta} \bar{f} e_\mu^a \tilde{\gamma}_a f = 0, \tag{2.25}$$

and those for the W_μ^i fields are found to be

$$g_E^{\mu\alpha} g_E^{\nu\beta} D_\alpha W_{\mu\nu}^i - g g_E^{\mu\beta} g_E^{\nu\sigma} \sum_{j,k=1}^{3} \epsilon_{ijk} W_{\mu\nu}^j W_\sigma^k - \frac{g}{4} g_E^{\mu\beta} e^{-\sqrt{\frac{2}{3}} \frac{\phi}{M_P}} h^2 \mathcal{W}_\mu^i + \frac{ig}{2} e^{-\sqrt{\frac{2}{3}} \frac{\phi}{M_P}} g_E^{\mu\beta} \bar{f} e_\mu^a \tilde{\gamma}_a \tau^i f = 0,$$

$$\text{with} \quad \mathcal{W}_\mu^i = \begin{cases} g W_\mu^i, & \text{if } i = 1,2 \\ g W_\mu^3 - g' B_\mu, & \text{if } i = 3 \end{cases}. \tag{2.26}$$

We define W_μ, Z_μ and A_μ in the usual way

$$W_\mu = \frac{W_\mu^1 - i W_\mu^2}{\sqrt{2}}, \qquad W_\mu^\dagger = \frac{W_\mu^1 + i W_\mu^2}{\sqrt{2}}$$

$$A_\mu = \sin\theta_W W_\mu^3 + \cos\theta_W B_\mu,$$

$$Z_\mu = \cos\theta_W W_\mu^3 - \sin\theta_W B_\mu, \tag{2.27}$$

with $e = g \sin\theta_W = g' \cos\theta_W$, and electroweak angle θ_W. We can express the W_μ^i and B_μ fields in terms of W_μ, Z_μ and A_μ by inverting the above equations.

Given that we are in the broken phase, for which $h_0 \neq 0$, where h_0 is the homogeneous background field as we shall see shortly, we can consider the trivial solution $\mathcal{W}_\mu^i = 0$ from the mass term in Eq. (2.26) as the variation is small compared to the background field. This means that we can set $W_\mu = W_\mu^\dagger = 0$ and $Z_\mu = \cos\theta_W W_\mu^3 - \sin\theta_W B_\mu = 0$ which implies that $B_\mu = \cos\theta_W A_\mu$ and $W_\mu^3 = \sin\theta_W A_\mu$. We will therefore retain only the photon field A_μ, replacing B_μ with $\cos\theta_W A_\mu$ in the corresponding Chern-Simons term. Put differently, the production of photon fields proceeds unsuppressed compared to the other heavy gauge bosons.

We now turn to some comments related to the gauge fixing in Eq. (2.5). The Higgs doublet contains, apart from the radial degree of freedom h, three Goldstone bosons $\vec{\chi}$. Using $SU(2)_L$ gauge invariance, and fixing the corresponding gauge parameter $\vec{\alpha}(x)$ as $\vec{\alpha}(x) = -\vec{\chi}(x)$ (unitary gauge), the Goldstone bosons disappear from the Lagrangian and the Higgs doublet reduces to Eq. (2.5). There is still the $U(1)$ gauge invariance that can be used to fix the Coulomb gauge for the electromagnetic field

$\partial^i A_i = 0$. This is done by fixing the hypercharge gauge field B_μ as $\partial^i B_i = -\tan\theta_W \partial^i W_i^3$. Moreover, in regions where the electric charge density is zero, it turns out that $A_0 = 0$ (the radiation gauge we use in this paper). Therefore, the EoM for the A_μ field simplifies to

$$g_E^{\mu\alpha} g_E^{\nu\beta} D_\alpha F_{A\mu\nu} + \frac{8\cos^2\theta_W M_P^2}{\xi_R \Lambda^2} \partial_\alpha \left(F(\phi^I) e^{\sqrt{\frac{2}{3}} \frac{\phi}{M_P}} \right) \tilde{F}_A^{\alpha\beta}$$

$$= ie Q_f e^{-\sqrt{\frac{2}{3}} \frac{\phi}{M_P}} g_E^{\mu\beta} \bar{f} e_\mu^a \tilde{\gamma}_a f, \tag{2.28}$$

with $Q_f = \frac{1}{2} Q_{Y_f} + T_{3f}$, where T_3 is the third component of weak isospin.

Similarly, one can find the general covariant Dirac equation as

$$g_E^{\mu\nu} e_\mu^a \tilde{\gamma}_a (\nabla_\nu^f f) = 0. \tag{2.29}$$

III. INFLATIONARY DYNAMICS IN THE COVARIANT FORMALISM

We now study the inflationary dynamics of our two-field scenario with the noncanonical kinetic term (i.e., with a nontrivial field-space manifold) following the covariant formalism discussed in Refs. [33,75,76] (see also Refs. [31,77–88]). Focussing on linear order perturbations, we decompose the fields into classical background (φ^I) and perturbation parts ($\delta\phi^I$) as

$$\phi^I(x^\mu) = \varphi^I(t) + \delta\phi^I(x^\mu), \tag{3.1}$$

with $\varphi^I(t) = \{\varphi(t), h_0(t)\}$. The space-time dynamics can be described by the perturbed spatially flat Friedmann-Robertson-Walker (FRW) metric, which is expanded as [89–91]

$$ds^2 = -(1 + 2\mathcal{A})dt^2 + 2a(t)(\partial_i\mathcal{B})dx^i dt + a(t)^2[(1 - 2\psi)\delta_{ij}$$
$$+ 2\partial_i\partial_j\mathcal{E}]dx^i dx^j. \qquad (3.2)$$

$a(t)$ denotes the scale factor, t parametrizes cosmic time, and $\mathcal{A}$, $\mathcal{B}$, ψ, and $\mathcal{E}$ characterize the scalar metric perturbations. Like the scalar fields, the space-time metric is also considered up to first order in the perturbations. In the following, when deriving the background and perturbation equations for scalar and gauge fields, we shall adopt the longitudinal gauge, i.e., $\mathcal{B} = \mathcal{E} = 0$.

One may define covariant field fluctuations $\mathcal{Q}^I$ (covariant with respect to the field-space metric) that connect $\phi^I(x^\mu)$ and $\varphi^I(t)$ along the geodesic of the field-space manifold with affine connection κ. Concretely, we can take $\phi^I(\kappa = 0) = \varphi^I$, $\phi^I(\kappa = \kappa') = \varphi^I + \delta\phi^I$ and $D_\kappa\phi^I|_{\kappa=0} = d\phi^I/d\kappa|_{\kappa=0} \equiv \mathcal{Q}^I$, such that with these conditions, the unique field-space vector $\mathcal{Q}^I$ connects ϕ^I and φ^I [75]. Note here, that D_κ is the covariant derivative with respect to the affine connection. The field fluctuations $\delta\phi^I$ can be expressed in a series of $\mathcal{Q}^I$ as [75,85]

$$\delta\phi^I = \mathcal{Q}^I - \frac{1}{2}\Gamma^I_{JK}\mathcal{Q}^J\mathcal{Q}^J + \frac{1}{3!}(\Gamma^I_{MN}\Gamma^N_{JK} - \Gamma^I_{JK,M})$$
$$\times \mathcal{Q}^I\mathcal{Q}^J\mathcal{Q}^M + ..., \qquad (3.3)$$

where the Christoffel symbols Γ^I_{JK} are evaluated at the background field order. The field fluctuations $\delta\phi^I(x^\mu)$ are gauge-dependent quantities under both the field-space transformation $\varphi^I \to \varphi'^I$, as well as the space-time transformation $x^\mu \to x'^\mu$. This is motivation to formulate gauge-independent Mukhanov-Sasaki variables, which are a linear combinations of space-time metric perturbation ψ and covariant field fluctuations $\mathcal{Q}^I$ as [90,92,93]

$$Q^I = \mathcal{Q}^I + \frac{\dot\varphi^I}{H}\psi. \qquad (3.4)$$

We remark that, while φ^I is not a vector of the field-space manifold, $\mathcal{Q}^I$, $\dot\varphi^I$ and Q^I all transform, indeed, as vectors of the field-space manifold. The Q^I is doubly covariant with respect to both space-time and field-space transformations to first order in the perturbations. It is useful to define the covariant derivative of vectors S^I and S_I in the field-space as

$$\mathcal{D}_J S^I \equiv \partial_J S^I + \Gamma^I_{JK}S^K, \qquad \mathcal{D}_J S_I \equiv \partial_J S_I - \Gamma^K_{IJ}S_K. \quad (3.5)$$

It is convenient to also define a covariant derivative with respect to cosmic time t

$$\mathcal{D}_t S^I \equiv \dot\varphi^J \mathcal{D}_J S^I = \dot{S}^I + \Gamma^I_{JK}S^J\dot\varphi^K, \qquad (3.6)$$

see also Refs. [83,84,94–96].

We turn to the stress-energy tensor $T_{\mu\nu}$, which can be written for the homogeneous, isotropic and spatially flat metric $\tilde{g}_{E\mu\nu} = \text{diag}(-1, a^2(t), a^2(t), a^2(t))$ as

$$T_{\mu\nu} = (p + \rho)U_\mu U_\nu + pg_{\mu\nu}, \qquad (3.7)$$

with a choice of $U_\mu = (1, 0, 0, 0)$ for the fluid four-velocity. For a spatially flat metric, employing Eq. (3.7) and the Einstein equations, we get the Friedmann equations for the background order

$$H^2 = \left(\frac{\dot a}{a}\right)^2 = \frac{1}{3M_P^2}\rho, \quad \text{and} \quad \dot H = -\frac{1}{2M_P^2}(p + \rho), \quad (3.8)$$

where p and ρ are pressure and energy density, respectively. We can compare the 00 and ij component of Eqs. (2.24) and (3.7) to get expressions for pressure p and energy density ρ,

$$\rho = T_{00}, p = \frac{1}{3a^2}\sum_{i=1}^{3}T_{ii}. \qquad (3.9)$$

At the considered background order, employing the explicit expression of Eq. (C5) (see Appendix C), the (inflaton) pressure and energy density reduce to

$$\rho = \frac{1}{2}G_{IJ}\dot\varphi^I\dot\varphi^J + V_0(\varphi^I), \qquad (3.10a)$$

$$p = \frac{1}{2}G_{IJ}\dot\varphi^I\dot\varphi^J - V_0(\varphi^I), \qquad (3.10b)$$

yielding the equation of state

$$w = \frac{p}{\rho} = \frac{G_{IJ}\dot\varphi^I\dot\varphi^J - 2V_0}{G_{IJ}\dot\varphi^I\dot\varphi^J + 2V_0}. \qquad (3.11)$$

Furthermore, the Hubble parameter and its derivative with respect to cosmic time take the form

$$H^2 = \left(\frac{\dot a}{a}\right)^2 = \frac{1}{3M_P^2}\left(\frac{1}{2}G_{IJ}\dot\varphi^I\dot\varphi^J + V_0(\varphi^I)\right), \quad (3.12a)$$

$$\dot H = -\frac{1}{2M_P^2}(G_{IJ}\dot\varphi^I\dot\varphi^J). \qquad (3.12b)$$

The EoMs for the background fields φ^I and the perturbations Q^I at linear order can be derived utilizing Eqs. (3.4) and (2.21)

$$\mathcal{D}_t\dot\varphi^I + 3H\dot\varphi^I + G^{IJ}V_{0,J} = 0, \qquad (3.13a)$$

$$\mathcal{D}_t^2 Q^I + 3H\mathcal{D}_t Q^I + \frac{k^2}{a^2}\delta_J^I Q^J + \mathcal{M}_L^I Q^L = 0, \quad (3.13\text{b})$$

with

$$\mathcal{M}_L^I = G^{IJ}(\mathcal{D}_L \mathcal{D}_J V_0) - \mathcal{R}_{JKL}^I \dot{\varphi}^J \dot{\varphi}^K - \frac{1}{M_{\text{P}}^2 a^3}\mathcal{D}_t\left(\frac{a^3}{H}\dot{\varphi}^I \dot{\varphi}_L\right),$$
$$(3.14)$$

and the field-space Riemann tensor $\mathcal{R}_{JKL}^I$. All relevant quantities such as V_0, G^{IJ}, Γ_{JK}^I, $\mathcal{R}_{JKL}^I$ in Eqs. (3.13) are evaluated at background order. Moreover, as the field-space metric G^{IJ} and M^{IJ} are diagonal in this approximation, the first-order perturbations do not mix the different Q^I. Note also that the EoMs for background and perturbations do not depend on the gauge fields for our linear-order considerations.

To study perturbations, we can find a set of unit vectors that differentiate between adiabatic and entropy directions. Firstly, we define the length of the velocity vector $\dot{\varphi}^I$ in field-space defined as

$$\dot{\sigma} = \sqrt{G_{IJ}\dot{\varphi}^I \dot{\varphi}^J} = \sqrt{\rho + p} \quad (3.15)$$

and the corresponding unit vector

$$\hat{\sigma}^I = \frac{\dot{\varphi}^I}{\dot{\sigma}}. \quad (3.16)$$

With this, we can rewrite Eq. (3.13a) to reproduce a single-field model with a canonically normalized kinetic term. The slow-roll parameters ϵ and η are

$$\epsilon = -\frac{\dot{H}}{H^2} = \frac{3\dot{\sigma}^2}{\dot{\sigma}^2 + 2V_0}, \quad (3.17\text{a})$$

$$\eta = M_{\text{P}}^2 \frac{\mathcal{M}_{\sigma\sigma}}{V_0}, \quad (3.17\text{b})$$

with $\mathcal{M}_{\sigma\sigma} \equiv \hat{\sigma}_I \hat{\sigma}^J \mathcal{M}_J^I = \hat{\sigma}^I \hat{\sigma}^J(\mathcal{D}_I \mathcal{D}_J V_0)$. Inflation ends when the slow-roll parameter reaches $\epsilon = 1$, and we denote the corresponding cosmological time as t_{end} in the following.

The field-space directions orthogonal to $\hat{\sigma}^I$ are given by

$$\hat{s}^{IJ} = G^{IJ} - \hat{\sigma}^I \hat{\sigma}^J, \quad (3.18)$$

and $\hat{\sigma}^I$ and $\hat{s}^{IJ}$ tensors are related by relations [31]

$$\hat{\sigma}^I \hat{\sigma}_I = 1, \quad \hat{s}^{IJ}\hat{s}_{IJ} = N - 1, \quad \hat{\sigma}_I \hat{s}^{IJ} = 0 \text{ for each } J. \quad (3.19)$$

$N = 2$, and $I, J = 1, 2$ in our two-field scenario. We can now decompose the perturbations in the directions of $\hat{\sigma}^I$ and $\hat{s}^{IJ}$ as

$$Q_\sigma = \hat{\sigma}_I Q^I, \quad (3.20)$$

$$\delta s^I = \hat{s}^I{}_J Q^J, \quad (3.21)$$

with Q_σ and δs^I being referred to as adiabatic and entropy perturbations, respectively. We also define a "turning vector" ω^I as the covariant rate of change of $\hat{\sigma}^I$,

$$\omega^I = \mathcal{D}_t \hat{\sigma}^I. \quad (3.22)$$

The turning vector is orthogonal with respect to $\hat{\sigma}^I$, $\omega_I \hat{\sigma}^I = 0$, the corresponding unit vector is

$$\hat{\omega}^I = \frac{\omega^I}{\omega}, \quad (3.23)$$

with $\omega = |\omega^I| = \sqrt{G_{IJ}\omega^I \omega^J}$.

With these definitions in place, we can now define the entropy perturbations as

$$Q_s = \hat{\omega}_I Q^I, \quad (3.24)$$

which are conveniently normalized to give

$$S = \frac{H}{\dot{\sigma}}Q_s. \quad (3.25)$$

The gauge-invariant curvature (adiabatic) perturbation $\mathcal{R}$ [90,91,97]

$$\mathcal{R} = \psi - \frac{H}{\rho + p}\delta q, \quad (3.26)$$

with ρ, p as defined above, and δq given by $\partial_i \delta q = -T_{0i}$ evaluated at background order (cf. Appendix C) together with Eqs. (3.3) and (3.4)

$$\delta q = -G_{IJ}\dot{\varphi}^I \delta\phi^J = -\dot{\sigma}\hat{\sigma}_I\left(Q^I - \frac{\dot{\varphi}^I}{H}\psi\right). \quad (3.27)$$

Therefore, $\mathcal{R}$ takes the compact form

$$\mathcal{R} = \psi + \frac{H}{\dot{\sigma}^2}\dot{\sigma}\hat{\sigma}_I\left(Q^I - \dot{\sigma}\frac{\hat{\sigma}^I}{H}\psi\right) = \frac{H}{\dot{\sigma}}Q_\sigma, \quad (3.28)$$

at linear order. In the presence of entropy perturbations, the gauge-invariant curvature perturbation does not need to be conserved, $\dot{\mathcal{R}} \neq 0$. The nonadiabatic pressure perturbation is given by [91,97]

$$\delta p_{\text{nad}} = \delta p - \frac{\dot{p}}{\dot{\rho}}\delta\rho = -\frac{2\hat{\sigma}^I \partial_I V}{3H\dot{\sigma}}\epsilon_m + 2\dot{\sigma}(\omega_I \delta s^I). \quad (3.29)$$

with ϵ_m as the comoving density perturbation. For super-horizon scales $k \ll aH$, the only source of nonadiabatic pressure stems from δs^I. This means that $\dot{\mathcal{R}} \neq 0$ will not vanish even at the $k \ll aH$ scale and $\omega_I \delta s^I$ will source Q_σ and hence $\dot{\mathcal{R}}$.

The gauge invariant curvature perturbation is defined as [90,97]

$$\langle \mathcal{R}(\boldsymbol{k}_1) \mathcal{R}(\boldsymbol{k}_2) \rangle = (2\pi)^3 \delta^{(3)}(\boldsymbol{k}_1 + \boldsymbol{k}_2) P_{\mathcal{R}}(t; k_1) \quad (3.30)$$

and $P_{\mathcal{R}}(t; k) = |\mathcal{R}|^2$. The dimensionless power spectrum for the adiabatic perturbation is given by

$$\mathcal{P}_{\mathcal{R}}(t; k) = \frac{k^3}{2\pi^2} |\mathcal{R}|^2. \quad (3.31)$$

Similarly, the power spectrum for the entropy perturbations is

$$\mathcal{P}_{\mathcal{S}}(t; k) = \frac{k^3}{2\pi^2} |\mathcal{S}|^2. \quad (3.32)$$

To find the power spectra of the curvature and isocurvature (entropy) perturbations, Eqs. (3.31) and (3.32), we utilize the quantities H, ϵ and unit vectors such as $\hat{\sigma}^I$, $\hat{\omega}^I$,…, from the solutions of the Eqs. (3.12a) and (3.13a) while Q_σ and Q_s are evaluated using the solutions of mode equations from Eq. (3.13b). For a given Fourier mode k, we calculate the different power spectra at the $t = t_{\text{end}}$ numerically as a function of k as

$$\mathcal{P}_{\mathcal{R}}(k) = \mathcal{P}_{\mathcal{R}}(t_{\text{end}}; k), \qquad \mathcal{P}_{\mathcal{S}}(k) = \mathcal{P}_{\mathcal{S}}(t_{\text{end}}; k), \quad (3.33)$$

where t_{end} denotes the time when inflation ends, i.e. when $\epsilon = 1$.

The spectral index n_s of the power spectrum of the curvature perturbation is defined as

$$n_s = 1 + \frac{d \ln \mathcal{P}_{\mathcal{R}}(k)}{d \ln k}. \quad (3.34)$$

As we will discuss in the next section, although our scenario involves scalar fields h and ϕ, we shall primarily focus on a scenario where the dynamics are essentially described by single fieldlike inflation. In such a case, the spectral index can be calculated as

$$n_s(t_*) \approx 1 - 6\epsilon(t_*) + 2\eta(t_*), \quad (3.35)$$

where t_* denotes the time when the reference scale exited the horizon and the tensor-to-scalar ratio is given by $r \approx 16\epsilon$.

TABLE I. Benchmark points chosen for our analysis. Scales are given in units of the Planck mass M_{P}. See text for details.

BP	ξ_R	ξ_H	$\varphi(t_{\text{in}})$ [M_{P}]	$h_0(t_{\text{in}})$ [M_{P}]
a	2.35×10^9	10^{-3}	5.5	2×10^{-4}
b	2.55×10^9	1	5.5	8.94×10^{-4}
c	2.2×10^9	10	5.4	5.00×10^{-3}

We choose three benchmark points to highlight quantitatively the implications of consistent inflation parameter choices when contextualized with baryogenesis. These are summarized in Table I alongside the required initial field values to satisfy Planck 2018 measurements: At the pivot scale $k = k_*$, the amplitude of $\mathcal{P}_{\mathcal{R}}(k)$ should match the scalar amplitude measurement of Ref. [4]

$$A_s = (2.099 \pm 0.014) \times 10^{-9} \quad \text{at } 68\% \text{ CL.} \quad (3.36)$$

As a guideline for our parameter choices and the initial values of the background fields, we follow the valley approximation that we discuss in Appendix D. We note that, while finding the parameter sets, we also ensure that the isocurvature mode remains orders of magnitude smaller than the curvature perturbation. The background equations are solved with initial conditions $\varphi(t_{\text{in}})$ and $h_0(t_{\text{in}})$ as in Table I, with vanishing time derivatives; t_{in} denotes the initial time for our numerical analysis in the following. The perturbation equations (3.13b) are solved with approximate initial conditions for a Fourier mode k

$$Q^I(t) \simeq \frac{H}{\sqrt{2k^3}} \left(i + \frac{k}{aH} \right) \exp\left\{ i \frac{k}{aH} \right\}, \quad (3.37)$$

sufficiently in the past such that the Hubble parameter at t_{in} remains approximately constant. In practice, we initialize the Q^I and their derivatives about four e-foldings before they exit the horizon for each mode.

In Fig. 1, we show the evolution of power spectra $\mathcal{P}_{\mathcal{R}}$ and $\mathcal{P}_{\mathcal{S}}$ (for the pivot scale $k = k_*$) and the spectral index n_s for BPa. Note, when calculating both power spectra, we solve Eqs. (3.31) and (3.32) numerically without any assumption related to slow-roll. It is clear from Fig. 1 that the isocurvature mode is orders of magnitude smaller than the adiabatic mode and both power spectra freeze out once they exit the horizon. We remark that while finding the power spectrum we always check the orthogonality conditions of Eq. (3.19) in our numerical analysis. In the following, we interchangeably use the cosmological time t and the number of e-foldings before the end of inflation which is defined as
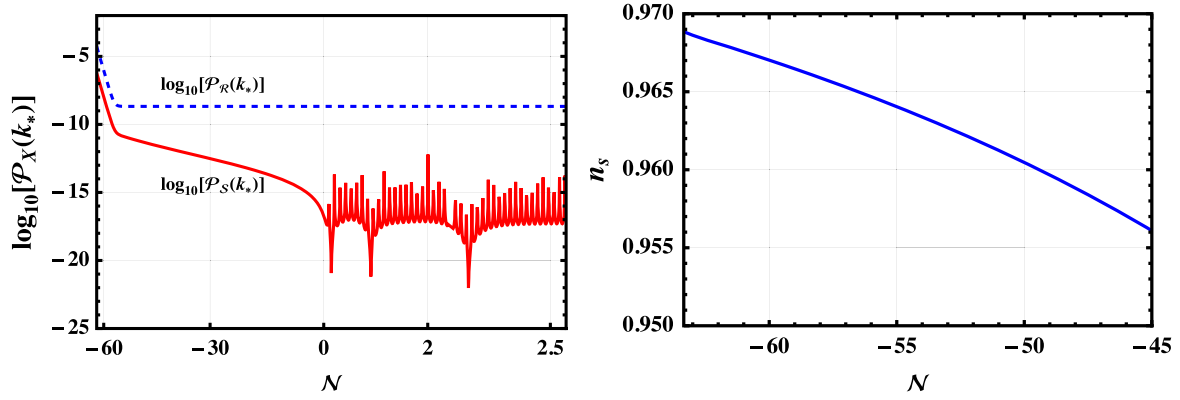
FIG. 1. The power spectra of the adiabatic and isocurvature modes and the spectral index n_s for the parameter values of BPa in Table I.
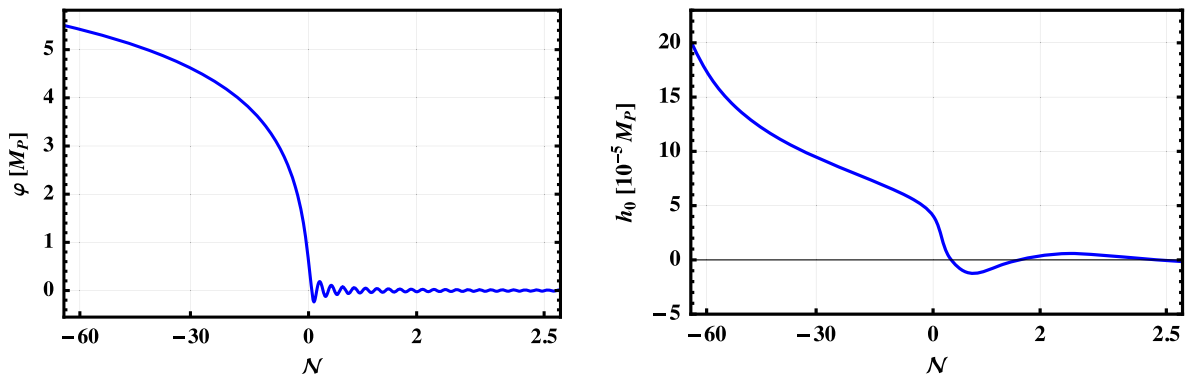

FIG. 2. The evolution of the background fields φ and the h_0 for the parameter values of BPa in Table I.

$$\mathcal{N} \equiv \ln \frac{a(t)}{a(t_{\text{end}})}. \qquad (3.38)$$

The pivot scale k_* exits the horizon $\mathcal{N}_* = 57, 59.3, 54.9 e$-foldings before the end of inflation for BPa, BPb, and BPc, respectively. For illustration, we also show the fields' time evolution in Fig. 2 for BPa, while, the evolution of

the Hubble parameter and the inflaton energy density are shown in Fig. 3. It is also clear from Fig. 1 that the spectral index n_s lies within the Planck 2018 range when the reference scale exits the horizon. The corresponding values of the tensor-to-scalar ratios are $r_* \sim 0.003$, which is consistent with expected values for R^2-Higgs inflation.
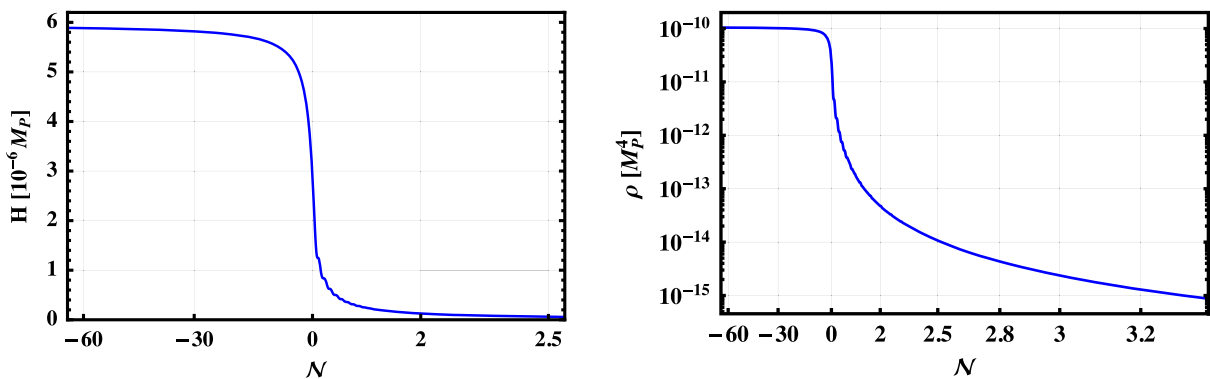

FIG. 3. The Hubble function H and the inflaton energy density ρ as in Eq. (3.10) for the parameter values of BPa given in Table I.

IV. GAUGE FIELD PRODUCTION

The EoM for the gauge field A_μ of Eq. (2.28) can be rewritten as

$$\frac{1}{\sqrt{-g_E}}\partial_\alpha\left(\sqrt{-g_E}g_E^{\mu\alpha}g_E^{\nu\beta}F_{A\mu\nu}\right)+\frac{8\cos^2\theta_W M_P^2}{\xi_R\Lambda^2}$$
$$\times\partial_\alpha(F(\phi^I)e^{\sqrt{\frac{2}{3}}\frac{\phi}{M_P}})\tilde{F}_A^{\alpha\beta}$$
$$-ieQ_f e^{-\sqrt{\frac{2}{3}}\frac{\phi}{M_P}}g_E^{\mu\beta}\bar{f}e_\mu^a\tilde{\gamma}_a f=0,\tag{4.1}$$

without the presence of a torsion term $F_{A\mu\nu}=D_\mu A_\nu-D_\nu A_\mu=\partial_\mu A_\nu-\partial_\nu A_\mu$. One can identify the fermion current

$$j^\mu=\sum_f ieQ_f e^{-\sqrt{\frac{2}{3}}\frac{\phi}{M_P}}g_E^{\mu\nu}\bar{f}e_\nu^a\tilde{\gamma}_a f\tag{4.2}$$

that sources the Schwinger effect.

A. Neglecting the Schwinger effect

First, we consider the scenario without Schwinger effect, i.e., when the fermion current is negligible. This is possible if the fermion field values are small. One can now separate the space and time component of the A_μ field. The time component of Eq. (2.25) at linear order in the perturbations is

$$-\frac{1}{a^2}\partial_i(\partial_i A_0-\partial_0 A_i)=0,\tag{4.3}$$

which, in temporal gauge $A_0=0$, reduces to $\partial_i\dot{A}_i=0$. The spatial components of Eq. (2.25) are found to be

$$\ddot{A}_i+H\dot{A}_i-\frac{1}{a^2}\partial_j(\partial_j A_i-\partial_i A_j)-\frac{\xi H}{a}\epsilon^{ijk}(\partial_j A_k-\partial_k A_j)=0.\tag{4.4}$$

where

$$H=\frac{\dot{a}}{a},\quad \xi=\frac{4\cos^2\theta_W M_P^2}{\xi_R\Lambda^2 H}\partial_0\left(F(\varphi^I)e^{\sqrt{\frac{2}{3}}\varphi/M_P}\right).\tag{4.5}$$

In momentum space, using the notation $\mathbf{A}\equiv\vec{A}$

$$\mathbf{A}(t,\mathbf{x})=\int\frac{d^3\mathbf{k}}{(2\pi)^{3/2}}\tilde{\mathbf{A}}(t,\mathbf{k})e^{-i\mathbf{k}\cdot\mathbf{x}},\tag{4.6}$$

with $|\mathbf{k}|=k$, Eq. (4.4) reads

$$\ddot{\tilde{\mathbf{A}}}+H\dot{\tilde{\mathbf{A}}}+\frac{k^2}{a^2}\tilde{\mathbf{A}}+\frac{2i\xi H}{a}(\mathbf{k}\times\tilde{A})=0.\tag{4.7}$$

The $\tilde{\mathbf{A}}$ field can be written in terms of transverse components as

$$\tilde{\mathbf{A}}=\sum_{\lambda=\pm}\tilde{A}^\lambda(t,\mathbf{k})\hat{\epsilon}^\lambda(\mathbf{k}),\quad\text{with}\quad\mathbf{k}\cdot\hat{\epsilon}^\lambda(\mathbf{k})=0,$$
$$i\mathbf{k}\times\hat{\epsilon}^\lambda(\mathbf{k})=\lambda k\hat{\epsilon}^\lambda(\mathbf{k}).\tag{4.8}$$

so that, using conformal time τ (with $\partial_0=\partial_t=a^{-1}\partial_\tau$), the EoM for the transverse components becomes

$$\partial_\tau^2\tilde{A}^\lambda+\omega_\lambda^2\tilde{A}^\lambda=0,\tag{4.9}$$

with

$$\omega_\lambda^2(\tau,k)=k^2+2\lambda\xi Hak.\tag{4.10}$$

In order to quantize the gauge fields, we first integrate Eq. (4.9) by parts to get the action quadratic in the fields

$$S^\lambda=\int d\tau\mathcal{L}_\lambda=\int d\tau d^3\mathbf{k}\left[\frac{1}{2}|\partial_\tau\tilde{A}^\lambda|^2-\frac{1}{2}\omega_\lambda^2(\tau,k)|\tilde{A}^\lambda|^2\right].\tag{4.11}$$

As we deal with noncanonical kinetic terms, we apply the quantization procedure detailed in Ref. [98]. The canonical momentum of the transverse modes are

$$\pi_\lambda(\tau,\mathbf{k})=\frac{\delta\mathcal{L}_\lambda}{\delta(\partial_\tau\tilde{A}^\lambda(\tau,-\mathbf{k}))},\tag{4.12}$$

with the commutation relation expressed as

$$[\tilde{A}^\lambda(\tau,\mathbf{k}),\partial_\tau\tilde{A}^{\lambda'}(\tau,\mathbf{q})]=i\delta_{\lambda\lambda'}\delta(\mathbf{k}+\mathbf{q}).\tag{4.13}$$

The field operator $\tilde{A}^\lambda(\tau,\mathbf{k})$ can be written as creation and annihilation operators

$$\tilde{A}^\lambda(\tau,\mathbf{k})=\hat{a}_\mathbf{k}^\lambda u_k^\lambda(\tau)+\hat{a}_{-\mathbf{k}}^\lambda u_k^\lambda(\tau),\tag{4.14}$$

and the mode equations for the gauge fields are then

$$\ddot{u}^\lambda+H\dot{u}^\lambda+\frac{\omega_\lambda^2}{a^2}u^\lambda=0.\tag{4.15}$$

From these mode functions, we can compute the gauge observables, namely the magnetic and electric fields' energy densities, magnetic helicity and its derivative, defined as

$$\rho_B=\frac{1}{a^4}\int_{k_{\min}}^{k_c}dk\frac{k^4}{4\pi^2}\sum_\lambda|u^\lambda|^2,\tag{4.16a}$$

$$\rho_E=\frac{1}{a^4}\int_{k_{\min}}^{k_c}dk\frac{k^2}{4\pi^2}\sum_\lambda|\partial_\tau u^\lambda|^2,\tag{4.16b}$$
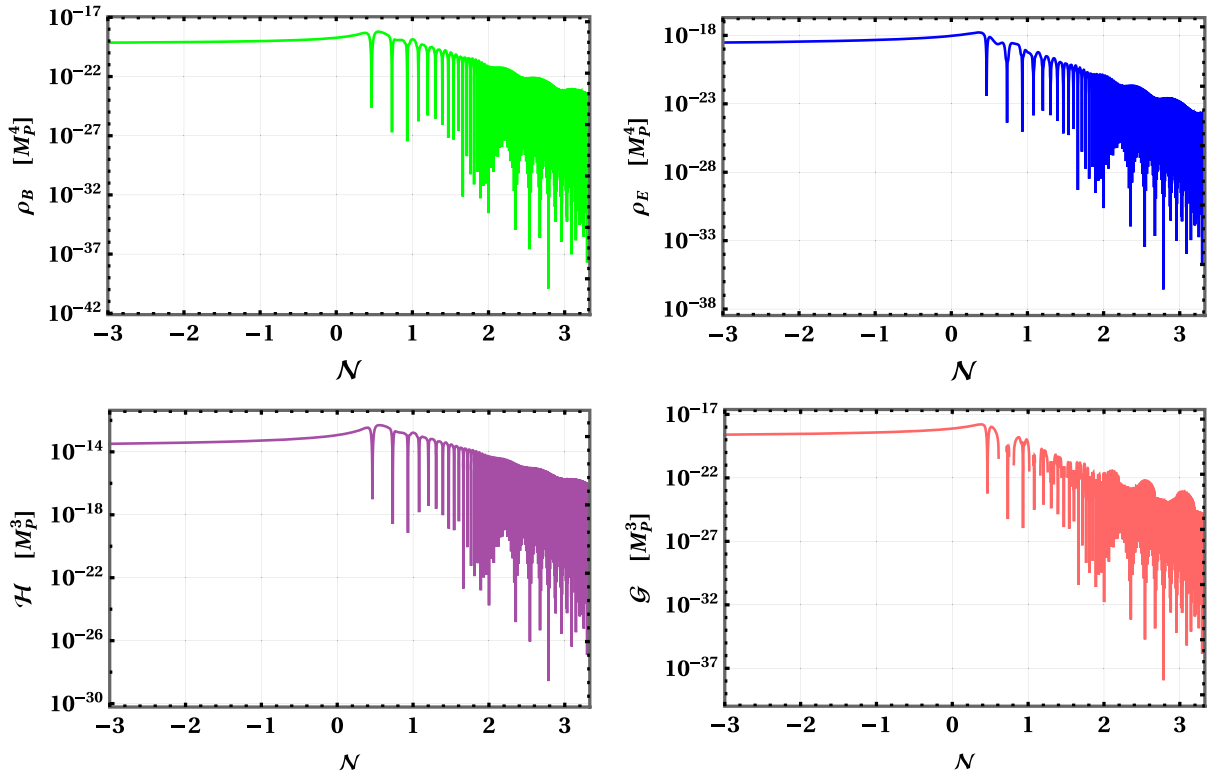
FIG. 4.   In the upper panel we plot the energy densities ρ_B and ρ_E with $\Lambda = 2.55 \times 10^{-5}\ M_P$ for the BPa summarized in Table I. The lower panel corresponds to the hyperhelical magnetic fields $\mathcal{H}$ and $\mathcal{G}$ for identical parameter choices.

$$\mathcal{H} = \frac{1}{a^3} \int_{k_{\min}}^{k_c} dk \frac{k^3}{2\pi^2} \left(|u^+|^2 - |u^-|^2 \right), \quad (4.16\text{c})$$

$$\mathcal{G} = \frac{1}{2} \frac{\partial \mathcal{H}}{\partial t}, \quad (4.16\text{d})$$

with the cutoff value given by [65,99]

$$k_c = 2|aH\xi|, \quad (4.17)$$

defined by the condition $\omega_\lambda^2(\tau, k_c) = 0$ satisfied by the helicity λ such that $\text{sign}(\lambda \xi) = -1$. The corresponding $U(1)_Y$ quantities are linked to the electromagnetic ones via

$$\begin{array}{ll} \rho_{B_Y} = \rho_B \cos^2\theta_W & \rho_{E_Y} = \rho_E \cos^2\theta_W \\ \mathcal{H}_Y = \mathcal{H} \cos^2\theta_W & \mathcal{G}_Y = \mathcal{G} \cos^2\theta_W \end{array} \quad (4.18)$$

In general, the integration limits should cover all modes from zero to infinity, however, not all modes are amplified during inflation. At the time t, the cut-off mode k_c is found by the solution of $\omega_\lambda = 0$; essentially this is when a mode $k = k_c$ crosses the horizon for the first time (at least for one helicity). The modes $k \gg k_c$ are not excited during inflation and can be neglected for the estimation of the above observable quantities. We will discuss $k_{\min}$ shortly.

In order to find ρ_B, ρ_E, $\mathcal{H}$ and $\mathcal{G}$ we solve Eq. (4.15) numerically via fourth-order Runge-Kutta (RK4) method in discrete time steps. We outline the details in Appendix E. For the ith time step, the gauge field modes are initialized with the Bunch-Davies (BD) initial condition as [100]

$$u_\lambda(k, t_i) \simeq \frac{1}{\sqrt{2k}} e^{-i\omega_i t_i}, \qquad \dot{u}_\lambda \simeq -i \frac{\omega_i}{\sqrt{2k}} e^{-i\omega_i t_i}, \quad (4.19)$$

with $\omega_i = ka^{-1}(t_i)$. It is practically not possible to go to the infinite past. Hence, to ensure that all modes remain well within the horizon at the initial time step t_{in}, we chose $k_{\min} = x_{\text{BD}} a(t_{\text{in}}) H(t_{\text{in}})$ with $x_{\text{BD}} = 100$. On the one hand, if a mode k remains well within the horizon, $k > x_{\text{BD}} a(t_i) H(t_i)$, we directly assume the BD solutions for the modes instead of applying the RK4 method for any subsequent time step. On the other hand, all superhorizon modes are solved with the RK4 method. For the numerical solution discussed below, we employ 25k time steps.

In Fig. 4, we show the evolution of ρ_B, ρ_E, $\mathcal{H}$ and $\mathcal{G}$ for BPa with $\Lambda = 2.55 \times 10^{-5}\ M_P$ for illustration. Similar values are found for the other benchmark points. We remark that we have compared our numerical results to the analytical approximation of the magnetic and electric fields' energy densities, magnetic helicity, and its derivative as in Ref. [65] and find good agreement.

B. Relevance of the Schwinger effect

We now turn to the impact of the Schwinger effect. The fermion current of Eq. (4.2) can be expressed as

$$j^\mu = (\rho_c, \boldsymbol{J}) \qquad (4.20)$$

The current and the gauge field are related by Ohm's law

$$\boldsymbol{J} = \sigma_c \boldsymbol{E} = -\sigma_c \partial_\tau \boldsymbol{A}, \qquad (4.21)$$

where the conductivity σ_c has been defined as a comoving quantity. The physical conductivity σ_{ph} relates to the comoving one via $\sigma_c = a\sigma_{ph}$. In the case of one Dirac fermion f with mass m_f and charge Q_f under a $U(1)$ group with coupling g, the comoving conductivity associated to f can be written as [71]

$$\sigma_f^c = \frac{|gQ_f|^3}{6\pi^2} \frac{a}{H} \sqrt{2\rho_B} \coth\left(\pi\sqrt{\frac{\rho_B}{\rho_E}}\right)$$

$$\times \exp\left\{-\frac{\pi m_f^2}{\sqrt{2\rho_E}|gQ_f|} - \sqrt{\frac{2}{3}}\frac{\varphi}{M_P}\right\}, \qquad (4.22)$$

where $m_f \equiv m_f(h_0) = m_f(v)h_0/v$ and so that

$$\sigma_c = \sum_f \sigma_f^c = \sum_\ell \sigma_\ell^c + N_c \sum_q \sigma_q^c, \qquad (4.23)$$

with $\ell = e, \mu, \tau$; $q = u, d, c, s, t, b$, $N_c = 3$ being the number of colors. Last, since we are in the broken phase, we identify g as the electric charge $g \equiv e \simeq 0.71$ at the scale in which inflation takes place.

This conductivity is to be distinguished from the conductivity of a thermal plasma after reheating in a radiation-dominated universe. We stress that the above is the conductivity at the end of inflation, before the reheating, produced by fermion pair formation from the magnetic field. Also, this estimation is valid in the case of collinear electric and magnetic fields, an assumption that we have numerically checked. Finally, the electric and magnetic fields are assumed to be slowly varying, as we expect the hypercharge gauge field to reach a stationary configuration, where the tachyonic instability and the induced current balance each other. We have verified in our numerical simulation that this is indeed the case.

In the presence of the fermion current, Eq. (4.7) becomes

$$\ddot{\tilde{\boldsymbol{A}}} + (H + \sigma_{ph})\dot{\tilde{\boldsymbol{A}}} + \frac{k^2}{a^2}\tilde{\boldsymbol{A}} + \frac{2iH\xi}{a}(\boldsymbol{k}\times\tilde{\boldsymbol{A}}) = 0, \quad (4.24)$$

which, for the transverse components in conformal time reads as

$$\partial_\tau^2 \tilde{A}^\lambda + \sigma_c \partial_\tau \tilde{A}^\lambda + \omega_\lambda^2 \tilde{A}^\lambda = 0, \qquad (4.25)$$

which can be recast as

$$\partial_\tau^2 \tilde{A}^\lambda + \left(\frac{\partial}{\partial\tau}\log(\Delta(\tau))\right)\partial_\tau \tilde{A}^\lambda + \omega_\lambda^2 \tilde{A}^\lambda = 0, \qquad (4.26)$$

with

$$\Delta(\tau) = \exp\left\{\int_{-\infty}^\tau \sigma_c(\tau')d\tau'\right\}. \qquad (4.27)$$

Integrating Eq. (4.26) by parts as in the previous subsection, one can now define the canonical momentum for the transverse modes as

$$\pi_\lambda(\tau,\mathbf{k}) = \frac{\delta\mathcal{L}_\lambda}{\delta(\partial_\tau \tilde{A}^\lambda(\tau,-\mathbf{k}))} = \Delta(\tau)\partial_\tau \tilde{A}^{\lambda'}(\tau,\mathbf{k}), \qquad (4.28)$$

and the commutation relation now becomes [98]

$$[\tilde{A}^\lambda(\tau,\mathbf{k}), \partial_\tau \tilde{A}^{\lambda'}(\tau,\mathbf{q})] = i\frac{1}{\Delta(\tau)}\delta_{\lambda\lambda'}\delta(\mathbf{k}+\mathbf{q}),$$

$$\text{with, } \tilde{A}^\lambda(\tau,\mathbf{k}) = \hat{a}_\mathbf{k}^\lambda u_k^\lambda(\tau) + \hat{a}_{-\mathbf{k}}^\lambda u_k^\lambda(\tau). \qquad (4.29)$$

The mode equations for the gauge fields in the presence of the Schwinger effect become

$$\ddot{u}^\lambda + (H + \sigma_c)\dot{u}^\lambda + \frac{k}{a}\left(\frac{k}{a} + 2\lambda H\xi\right)u^\lambda = 0, \qquad (4.30)$$

and the cut-off momenta k_c is now modified to

$$k_c = |aH\xi| + \sqrt{(aH\xi)^2 + \frac{a^2}{2}\left[\dot{\sigma}_{ph} + \sigma_{ph}\left(\frac{\sigma_{ph}}{2} + H\right)\right]}. \qquad (4.31)$$

At early times solution of the mode equations of Eq. (4.30) are represented by WKB solution [33,98]

$$u^\lambda(\tau) = \frac{1}{\sqrt{2}}\frac{1}{\sqrt{\Delta(\tau)\omega_\lambda(\tau,k)}}e^{-i\int_{\tau_{in}}^\tau d\tau'\omega_\lambda(\tau',k)} \qquad (4.32)$$

as long as $|\frac{\partial_\tau \omega_\lambda}{\omega_\lambda}| \ll 1$. In practice, we utilize the early-time solution for the modes

$$u^\lambda(\tau) = \frac{1}{\sqrt{2}}\frac{1}{\sqrt{\Delta(\tau)\omega_\lambda(\tau,k)}}e^{-ik\tau} \qquad (4.33)$$

to find relevant, observable quantities. From Eqs. (4.30) and (4.31), we find the energy densities for BPa and display them in the right panel of Fig. 5.

Due to the coupling between the fermion and gauge sectors, massless hypercharged fermions are continuously produced during inflation. They are massless as long as the
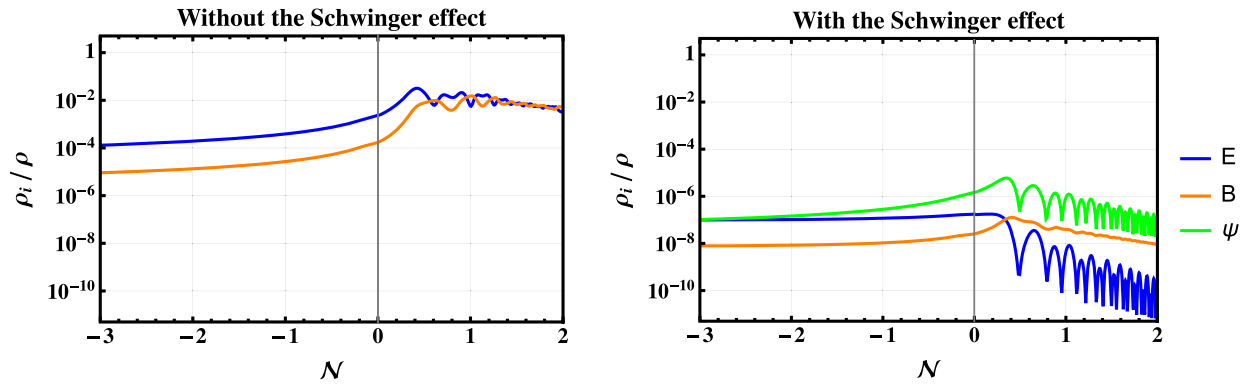
FIG. 5. Energy breakdown for $\xi_R = 2.35 \times 10^9$, $\xi_H = 10^{-3}$ and $\Lambda = 2 \times 10^{-5}\,M_P$ at the end of inflation and the onset of reheating. We show a comparison between the absence and the presence of the Schwinger effect for the quantities $\rho_i(\mathcal{N})/\rho(\mathcal{N})$, $i = E, B, \psi$. When the Schwinger effect is strong, like here, the fermion energy density can dominate over the gauge density. Still, all energy shares are reduced in the presence of the Schwinger effect.

EW symmetry remains intact and thus contribute to the energy density of relativistic radiation as

$$\rho_\psi = \lim_{V \to \infty} \frac{\sigma_c}{V} \int_V d^3x \frac{\langle \mathbf{A} \cdot \mathbf{E} \rangle}{a^4} = \frac{\sigma_c}{a^4} \int_{k_{\min}}^{k_c} dk \frac{k^2}{2\pi^2} \frac{d}{d\tau} \sum_\lambda |u^\lambda|^2.$$

(4.34)

It has been shown in Ref. [99] that the fermion energy density can easily dominate over the energy densities of E and B fields at the end of inflation. This situation has been chosen as an example in Fig. 5 where we display the energy fraction $\rho_i(\mathcal{N})/\rho(\mathcal{N})$, $i = E, B, \psi$ at the end of inflation and the onset of reheating. We show a direct comparison between the presence and the absence of the Schwinger effect. While for $\Lambda \gtrsim 4 \times 10^{-5} M_P$ the difference is an order one factor, the Schwinger effect reduces the amount of electromagnetic energy and helicity up to two orders of magnitude for $\Lambda \simeq 2.4 \times 10^{-5} M_P$, see Fig. 7. This is because the presence of the Schwinger effect trades an exponential behavior in ξ with a polynomial one.

When the gauge share dominates at least by 80%, the Universe will reheat before the perturbative decay of the inflaton [100], a phenomenon called *gauge preheating*. As in Ref. [65], we found that preheating is unlikely since the ratio is $\sim 10^{-6}$ at most. However, the huge damping in both energy and helicity does not preclude a window in the parameter space where the BAU is achieved, as we will see in the next section.

V. BARYOGENESIS

To generate a baryon asymmetry, the Sakharov conditions [51] must be met: (i) the system must contain a process that violates the baryon number, (ii), this process also violates C/CP symmetries, (iii) this process occurs out of thermal equilibrium. In the SM, the CP-violating term from the CKM matrix phase is too small to induce a

significant baryon asymmetry at a low energy scale, hence we included the dimension-six CP-odd term between Ricci scalar and $U(1)_Y$ gauge boson. On the other hand, in the symmetric phase of the EW plasma, the SM exhibits a chiral anomaly that is enough to source the present-day BAU. The anomaly expresses the fact that the $B + L$ anomaly, the $U(1)_Y$ helicity and the weak sphaleron are connected as

$$\Delta N_B = \Delta N_L = N_g \left(\Delta N_{\text{CS}} - \frac{g'^2}{16\pi^2} \Delta \mathcal{H}_Y \right). \quad (5.1)$$

The factor $N_g = 3$ is the number of fermion generations and g' is the $U(1)_Y$ gauge coupling. Under the thermal fluctuation of the $SU(2)_L$ gauge fields, the Chern-Simons number N_{CS} is diffusive, resulting in the rapid washout of both lepton N_L and baryon N_B numbers. On the contrary, a helical primordial magnetic field acts as a source, and a net baryon asymmetry can remain after the EW phase transition.

In Refs. [53,60], the effects of the helicity decay and sphaleron washout balance have been studied within a careful analysis of the transport equations for all SM species during the EWPT. As a result, a nonzero baryon-to-entropy ratio η_B remains in the broken phase while the transformation of baryon asymmetry back into helicity is avoided. The novelty of the mechanism lies in the introduction of a time-dependent (temperature-dependent) weak mixing angle $\theta_W(T)$ which enters an additional source of the baryon number into the kinetic equation. When the EW symmetry breaking occurs at $T \simeq 160$ GeV, the primordial hypermagnetic field becomes an electromagnetic field. However, the electroweak sphaleron remains in equilibrium until $T \simeq 130$ GeV and threatens to washout the baryon asymmetry. Therefore proper modeling of the epoch 160 GeV $\gtrsim T \gtrsim 130$ GeV is critical to an accurate prediction of the relic BAU.

The behavior of $\theta_W(T)$ is confirmed by analytic calculations [50], and numerical lattice simulations [101]. We follow Refs. [60,61] and model it with a smooth step function

$$\cos^2\theta_W = \frac{g^2}{g'^2 + g^2} + \frac{1}{2}\frac{g'^2}{g'^2 + g^2}\left(1 + \tanh\left[\frac{T - T_{\text{step}}}{\Delta T}\right]\right) \quad (5.2)$$

which, for $155 \text{ GeV} \lesssim T_{\text{step}} \lesssim 160 \text{ GeV}$ and $5 \text{ GeV} \lesssim \Delta T \lesssim 20 \text{ GeV}$, describes reasonably well the analytical and lattice results for the temperature dependence. Consequently, it is possible to generate the observed BAU from a maximally helical magnetic field that was generated before the EW crossover. Indeed, including all contributions, the Boltzmann equation for the baryon-to-entropy ratio η_B reads

$$\frac{d\eta_B}{dx} = -\frac{111}{34}\gamma_{W\,\text{sph}}\eta_B + \frac{3}{16\pi^2}(g'^2 + g^2)\sin(2\theta_W)\frac{d\theta_W}{dx}\frac{\mathcal{H}_Y}{s}, \quad (5.3)$$

where $x = T/H(T)$, with $H(T)$ being the Hubble rate at temperature T, $\mathcal{H}_Y$ the hypermagnetic helicity that is initially present and s the comoving entropy density of the SM plasma given by $s = (2\pi^2/45)g_* T^3$. Furthermore, $\gamma_{W\,\text{sph}} = 6\Gamma_{W\,\text{sph}}/T^4$ is the dimensionless transport coefficient for the EW sphaleron which, for temperatures $T < 161 \text{ GeV}$, is found from lattice simulations to be [102]

$$\gamma_{W\,\text{sph}} \simeq \exp\left\{-147.7 + 107.9\frac{T}{130 \text{ GeV}}\right\}. \quad (5.4)$$

The Boltzmann equation (5.3) has been numerically solved in Ref. [60] and the baryon-to-entropy ratio η_B was found to become frozen, i.e. $\dot{\eta}_B = 0$, at a temperature $T \simeq 135 \text{ GeV}$. As expected, this is close to the temperature $T \simeq 130 \text{ GeV}$ at which EW sphalerons freeze out. Setting the RHS of Eq. (5.3) to zero and solving for η_B yields

$$\eta_B \simeq 4 \times 10^{-12} f_{\theta_W}\frac{\mathcal{H}_Y}{H^3(t_{\text{end}})}\left(\frac{H(t_{\text{end}})}{10^{13} \text{ GeV}}\right)^{\frac{3}{2}}\left(\frac{T_{\text{rh}}}{T_{\text{rh}}^{\text{ins}}}\right), \quad (5.5)$$

where the (instant) reheating temperature is

$$T_{\text{rh}} = \left(\frac{90}{\pi^2 g_*}\right)^{\frac{1}{4}}\sqrt{\Gamma_\phi}, \qquad T_{\text{rh}}^{\text{ins}} = \left(\frac{90}{\pi^2 g_*}\right)^{\frac{1}{4}}\sqrt{H(t_{\text{end}})}, \quad (5.6)$$

and Γ_ϕ is the total decay width of the inflaton that reheats the universe after inflation.

All the details on the EWPT dynamics are encoded in the parameter f_{θ_W} which is subject to significant uncertainties

$$f_{\theta_W} = -\sin(2\theta_W)\frac{d\theta_W}{d\log T}\bigg|_{T = 135 \text{ GeV}},$$

$$5.6 \times 10^{-4} \lesssim f_{\theta_W} \lesssim 0.32. \quad (5.7)$$

The bounds on f_{θ_W} are given by varying T_{step} and ΔT in the ranges given below Eq. (5.2). The result Eq. (5.5) is a main ingredient of this work as it directly relates the amount of the final BAU to the amount of hypermagnetic helicity available at the EWPT.

The production of hypermagnetic fields nevertheless happens at the inflationary scale, hence one must ensure that the helicity is preserved as the Universe cools down in the radiation-dominated era that follows reheating. A rough estimate is to require that the magnetic Reynolds number $\mathcal{R}_m$ is bigger than unity, as this implies that the effects of magnetic induction are dominating over magnetic diffusion in the thermal plasma. On the other hand, the electric Reynolds number $\mathcal{R}_e$ determines in which regime the plasma evolves and informs us how to calculate the magnetic Reynolds number, see, e.g., Refs. [62,64]. In our work, we found that we are in the viscous regime, $\mathcal{R}_e < 1$, and hence we need to satisfy the constraint

$$\mathcal{R}_m^{\text{rh}} \approx 5.9 \times 10^{-6}\frac{\rho_{B_Y}\ell_{B_Y}^2}{H(t_{\text{end}})^2}\left(\frac{H(t_{\text{end}})}{10^{13} \text{ GeV}}\right)\left(\frac{T_{\text{rh}}}{T_{\text{rh}}^{\text{ins}}}\right)^{\frac{2}{3}} > 1, \quad (5.8)$$

where ℓ_{B_Y} is the hypermagnetic characteristic size given by

$$\ell_{B_Y} = \frac{2\pi}{\rho_B a^3}\int_{k_{\min}}^{k_c} dk \frac{k^3}{4\pi^2}\sum_\lambda |u^\lambda|^2. \quad (5.9)$$

The magnetohydrodynamics description of the plasma also admits a CP-odd term that can induce a helicity cancellation because of the fermion asymmetry back-transformation into helical gauge fields with opposite sign. This is because the energy configuration in the gauge sector is more favorable than in the fermion sector [103], a phenomenon called chiral plasma instability (CPI). Thus, one must ensure that all fermion asymmetry created alongside the helical field during inflation is erased by the action of the weak sphaleron for $10^{12} \text{ GeV} \gtrsim T \gtrsim 130 \text{ GeV}$. Because the weak interaction only couples to left-handed fermions, the right-handed fermions are protected from the washout until their Yukawa interaction becomes relevant in thermal equilibrium. The right-handed electron e_R is the last species to come into chemical equilibrium, at temperatures $\sim 10^5 \text{ GeV}$, thus its asymmetry survives the longest. Therefore, to efficiently erase the fermion asymmetry, while preserving the helicity in the gauge sector, before the CPI can happen, one must require that [62,103]
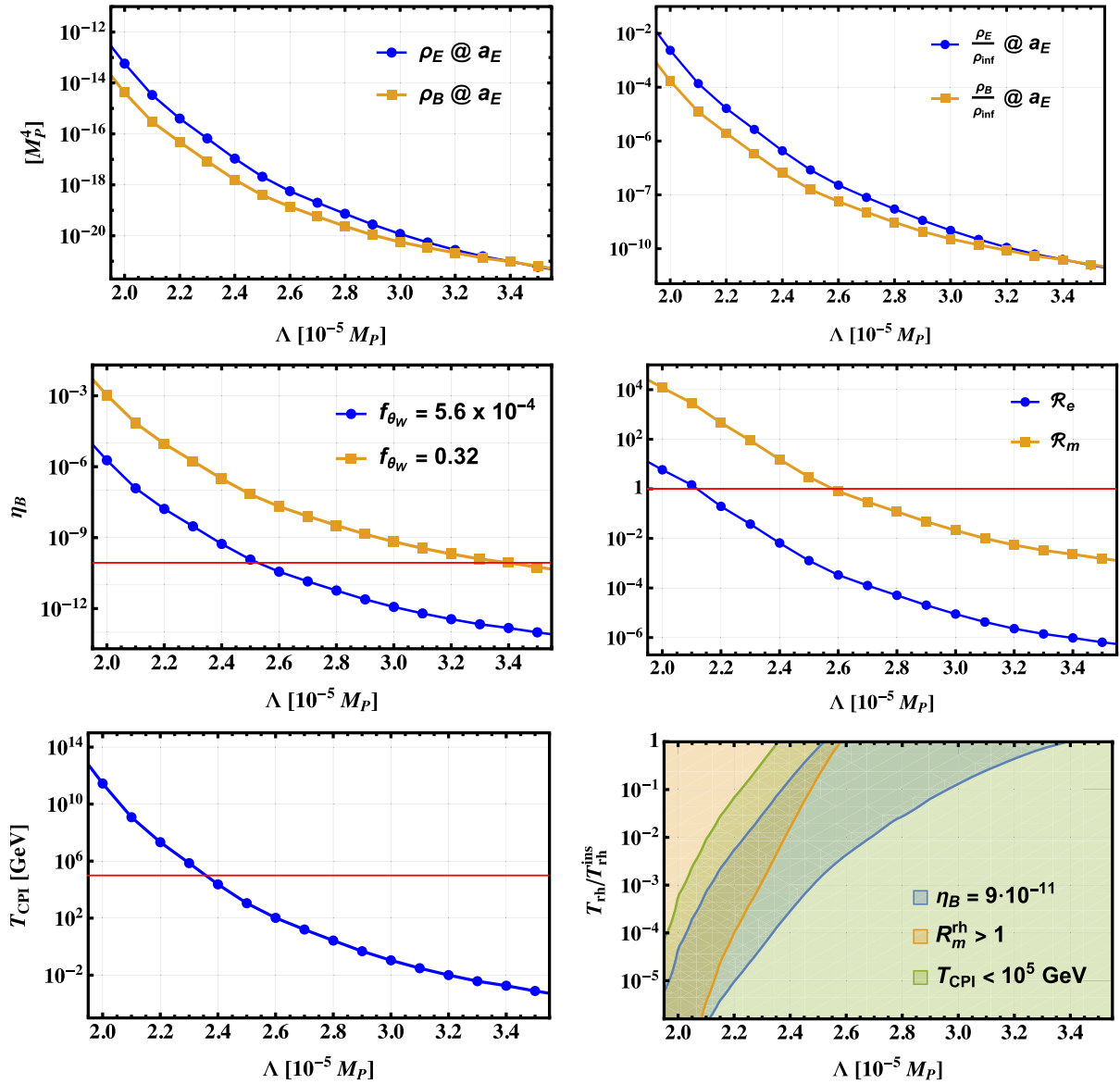
FIG. 6. These figures display a scan of the parameter Λ with the first set of initial conditions, see BPa in Table I without Schwinger effect. Top panels: magnetic and electric energy density (left) and their ratio with the inflation energy density (right). Middle panel: baryon asymmetry η_B (left) and Reynolds numbers (right) with their corresponding constraints in red. Bottom panels: CPI temperature with constraint in red (left) and baryogenesis parameter space (right).

$$T_{\mathrm{CPI}} \approx (4 \times 10^{-7}~\mathrm{GeV}) \frac{\mathcal{H}_Y^2}{H(t_{\mathrm{end}})^6} \left(\frac{H(t_{\mathrm{end}})}{10^{13}~\mathrm{GeV}} \right)^3 \left(\frac{T_{\mathrm{rh}}}{T_{\mathrm{rh}}^{\mathrm{ins}}} \right)^2$$

$$\lesssim 10^5~\mathrm{GeV}. \qquad (5.10)$$

In Figs. 6 and 7, we display the main results for the baryogenesis mechanism both in the presence and absence of the Schwinger effect. In both figures, the top panels display the electromagnetic energy and energy ratio to the background energy density. In the middle panels we show the quantities $\eta_B(\Lambda, f_{\theta_W})$, $\mathcal{R}_m(\Lambda)$ and $\mathcal{R}_e(\Lambda)$. On the left, the red line must be in between the two curves to meet the constraint. On the right, the only constraint is that $\mathcal{R}_m$ is

above the red line. Finally, at the bottom, we present the CPI temperature as a function of Λ and the regions where the different constraints are met. On the bottom left panel, the curve should be below the red line. On the right one, we shall seek the overlapping region. In this last plot, we add the temperature ratio $T_{\mathrm{rh}}/T_{\mathrm{rh}}^{\mathrm{ins}}$ as a supplementary parameter. We see that the window is larger in the presence of the Schwinger, which also totally removes the constraint on T_{CPI}. Indeed, the backreactionless mechanism tends to overshoot the BAU, an issue addressed by the presence of the Schwinger effect which therefore acts as a BAU facilitator.
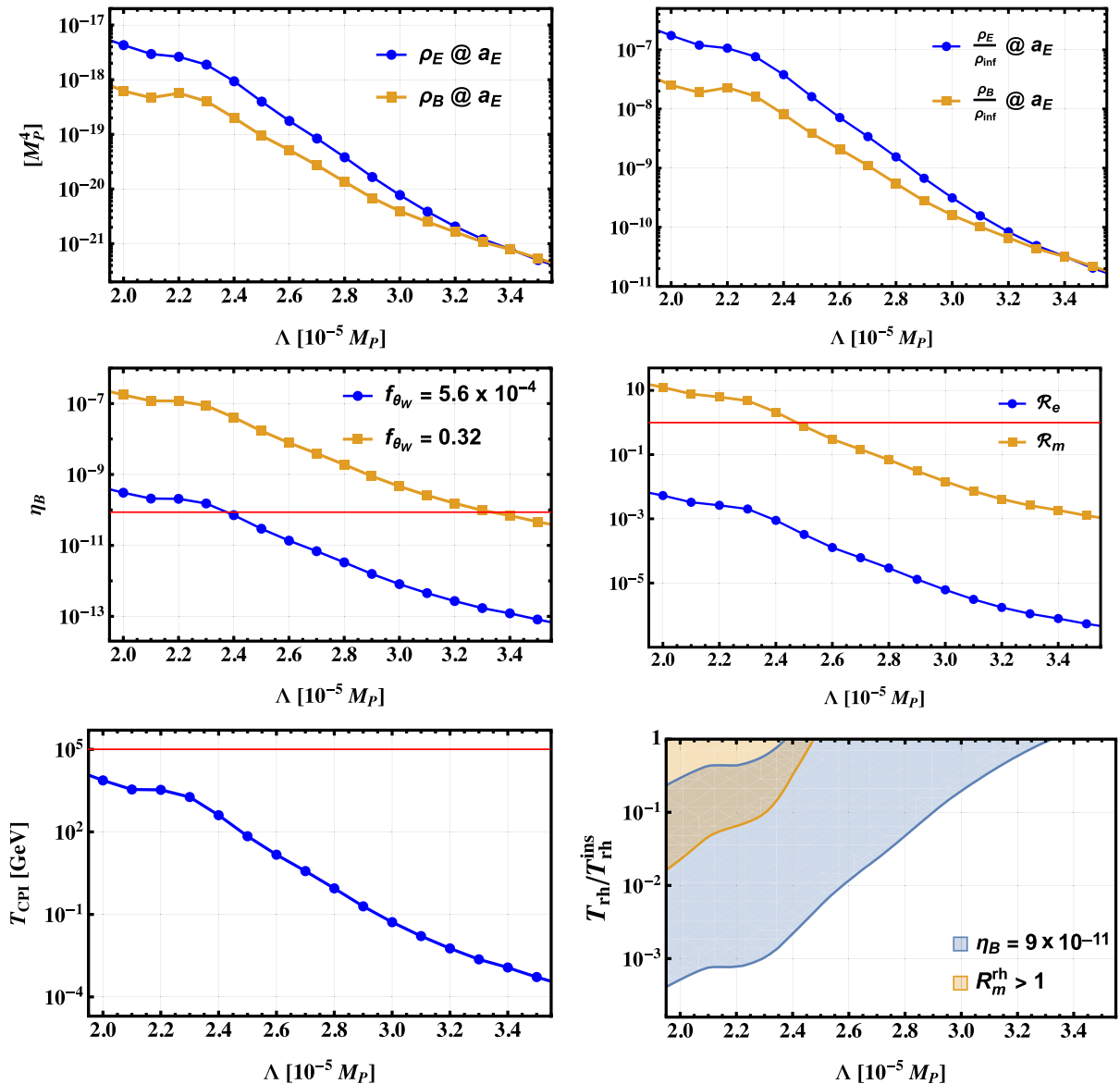
FIG. 7. Similar to Fig. 6, these figures again display a scan of the parameter Λ with the first set of initial conditions, BPa in Table I including the Schwinger effect. Top panels: Magnetic and electric energy density (left) and their ratio with the inflation energy density (right). Middle panel: baryon asymmetry η_B (left) and Reynolds numbers (right) with their corresponding constraints in red. Bottom panels: CPI temperature with constraint in red (left) and baryogenesis parameter space (right). We did not display the CPI temperature on this last plot as the CPI is no longer a constraint.

VI. SUMMARY AND CONCLUSIONS

We have discussed baryogenesis in the context of R^2-Higgs inflation, involving the CP-violating dimension-six term proportional to $(R/\Lambda^2)B_{\mu\nu}\tilde{B}^{\mu\nu}$. We adopt a fully covariant formalism for both inflationary dynamics and gauge field production. Our linear order analysis shows that if $\Lambda \sim 3 \times 10^{-5}~M_P$, sufficient helical hypermagnetic fields are produced, which can lead to the observed BAU during the electroweak crossover. Smaller values of Λ imply an overproduction of baryons. Once the Schwinger effect is included, the energy densities ρ_E and ρ_B are suppressed, but

there is a subtlety: the Schwinger effect is exponentially suppressed by a factor $\sim \exp(-\sqrt{(2/3)}\varphi/M_P)$, which dilutes its relevance during the inflationary epoch, but becomes pronounced around and after the end of inflation. The Schwinger effect can then lead to baryogenesis for smaller values $\Lambda \sim 2.2 \times 10^{-5}~M_P$. We also find that when the Schwinger effect is included, the radiation density ρ_ψ can dominate over the electromagnetic densities ρ_E and ρ_B, cf. Fig. 5.

We have primarily focused on the Starobinsky-like regime in our linear order analysis. In the mixed

R^2-Higgs scenario, a smaller Λ may generate BAU without the Schwinger effect. This can be understood from Eq. (2.25) where a smaller ξ_R and moderately large ξ_H (i.e. the mixed R^2-Higgs like regime) can induce inflation, while BAU can be triggered by a larger scale Λ. However, a larger ξ_H may lead to an exponential growth of isocurvature modes (see e.g. Refs. [78,104,105]) in our backreactionless scenario although such a mode is suppressed during inflation. Moreover, in such a scenario, one would need to take into account nonperturbative effects. In our analysis, we have not considered the impact of decay and self-resonance. Thus, the ratio $T_{\rm rh}/T_{\rm rh}^{\rm ins}$ is essentially a free parameter in our analysis. We leave a more detailed analysis of (p)reheating and particle production for future work. It has been pointed out that the helical gauge fields may source non-Gaussianity [106,107], which may result in moderate constraint to the parameter space for baryogenesis without the Schwinger effect [64]. In the presence of the Schwinger effect, the produced helical gauge fields are much weaker and we expect those constraints to be harmless. However, one needs to be careful when interpreting results from Refs. [106,107] as they focus on a single field. In our multi-field model, a proper estimation of non-Gaussianity requires considering perturbations up to third order. This would induce several new contributions from field-space Riemann tensor [76] and is beyond the scope of our work.

While there are many avenues to achieve the observed BAU, baryogenesis driven by a dimension-six CP-odd term $\sim (R/\Lambda^2)B_{\mu\nu}\tilde{B}^{\mu\nu}$ provides a motivated approach to address BAU within the framework of R^2-Higgs inflation. This approach critically rests on the presence of an effective dimension-six term, but it does not require additional degrees of freedom beyond the SM. In parallel, such dimension-six terms can also shed light on the UV sensitivity of R^2-Higgs inflation as discussed in, e.g., Refs. [108,109].

APPENDIX A: THE VIERBEIN FIELDS

The vierbein fields e_μ^a are defined as follows: The metric in the Jordan frame $g_{J\mu\nu}$ can be related at every point to a Minkowski tangent space η_{ab} via the vierbein, which obeys the following orthogonality conditions

$$e_\mu^a e_a^\nu = \delta_\mu^\nu, \qquad e_\mu^a e_b^\mu = \delta_b^a,$$
$$g_{J\mu\nu} = e_\mu^a e_\nu^b \eta_{ab} \quad \text{and} \quad \gamma_\mu = e_\mu^a \tilde{\gamma}_a, \qquad \text{(A1)}$$

where $\tilde{\gamma}_a$ are the Minkowski γ-matrices. The γ_μ satisfy $\{\gamma^\mu, \gamma^\nu\} = 2g_J^{\mu\nu}$ in curved space-time. The spin-affine connection is given by

$$\Gamma_\mu = \frac{1}{2}\omega_{\mu ab}\sigma^{ab} \quad \text{with} \quad \sigma^{ab} = \frac{1}{4}[\tilde{\gamma}^a, \tilde{\gamma}^b]. \qquad \text{(A2)}$$

The spin-connection $\omega_{\mu b}^a$ is defined as [110]

$$\omega_{\mu b}^a \equiv (e_\nu^a e_b^\beta \Gamma_{\mu\beta}^\nu - e_b^\beta \partial_\mu e_\beta^a). \qquad \text{(A3)}$$

APPENDIX B: FIELD-SPACE METRIC AND CHRISTOFFEL SYMBOLS

The field-space G^{IJ} metric is given by

$$G^{\phi\phi} = 1, \qquad G^{hh} = e^{\sqrt{\frac{2}{3}}\frac{\phi}{M_P}}, \qquad G^{\phi h} = G^{h\phi} = 0. \quad \text{(B1)}$$

The corresponding nonvanishing Christoffel symbols are therefore

$$\Gamma_{hh}^\phi = \frac{e^{-\sqrt{\frac{2}{3}}\frac{\phi}{M_P}}}{\sqrt{6}M_P}, \qquad \Gamma_{\phi h}^h = \Gamma_{h\phi}^h = -\frac{1}{\sqrt{6}M_P}. \qquad \text{(B2)}$$

APPENDIX C: EINSTEIN EQUATION AND STRESS-ENERGY TENSOR

The action S_E can be rewritten in the following way

$$S_E = \int d^4x \sqrt{-g_E}\left(\frac{M_P^2}{2}R_E + \mathcal{L}_M\right), \qquad \text{(C1)}$$

where $\mathcal{L}_M$ is all terms in the action other than R_E. Varying the action with respect to $g_E^{\mu\nu}$ we get

$$0 = \delta S_E$$

$$= \int d^4x \left(\frac{M_{\mathrm{P}}^2}{2} \frac{\delta(\sqrt{-g_E} R_E)}{\delta g_E^{\mu\nu}} + \frac{\delta(\sqrt{-g_E} \mathcal{L}_M)}{\delta g_E^{\mu\nu}} \right) \delta g_E^{\mu\nu}$$

$$= \int d^4x \left(\frac{M_{\mathrm{P}}^2}{2} \left(R_E \frac{\delta(\sqrt{-g_E})}{\delta g_E^{\mu\nu}} + \sqrt{-g_E} \frac{\delta(R_E)}{\delta g_E^{\mu\nu}} \right) + \sqrt{-g_E} \frac{\delta(\mathcal{L}_M)}{\delta g_E^{\mu\nu}} + \mathcal{L}_M \frac{\delta(\sqrt{-g_E})}{\delta g_E^{\mu\nu}} \right) \delta g_E^{\mu\nu}. \tag{C2}$$

Utilizing $\frac{\delta(\sqrt{-g_E})}{\delta g_E^{\mu\nu}} = -\frac{1}{2}\sqrt{-g_E} g_{E\mu\nu}$, $\frac{\delta(R_E)}{\delta g_E^{\mu\nu}} = R_{E\mu\nu}$ and ignoring the surface term we get

$$R_{E\mu\nu} - \frac{1}{2} g_{E\mu\nu} R_E = \frac{1}{M_{\mathrm{P}}^2} T_{\mu\nu} \tag{C3}$$

where

$$T_{\mu\nu} = \left(\mathcal{L}_M g_{E\mu\nu} - 2 \frac{\delta \mathcal{L}_M}{\delta g_E^{\mu\nu}} \right), \tag{C4}$$

which is found to be

$$T_{\mu\nu} = \left[G_{IJ} D_\mu \phi^I D_\nu \phi^J + g_E^{\alpha\beta} B_{\alpha\mu} B_{\beta\nu} + g_E^{\alpha\beta} W_{\alpha\mu}^i W_{\beta\nu}^i + \frac{1}{2} e^{-\sqrt{\frac{2}{3}}\frac{\phi}{M_{\mathrm{P}}}} g^2 h^2 \frac{(W_\mu^1 - iW_\mu^2)}{\sqrt{2}} \frac{(W_\nu^1 + iW_\nu^2)}{\sqrt{2}} \right.$$

$$+ \frac{2M_{\mathrm{P}}^2}{\xi_R \Lambda^2 \sqrt{-g_E}} F(\phi^I) e^{\sqrt{\frac{2}{3}}\frac{\phi}{M_{\mathrm{P}}}} \left(2 g_{E\mu\alpha} \epsilon^{\alpha\beta\rho\sigma} B_{\nu\beta} B_{\rho\sigma} + \frac{1}{8} g_{E\mu\nu} \epsilon^{\alpha\beta\rho\sigma} B_{\alpha\beta} B_{\rho\sigma} \right)$$

$$+ \frac{1}{4} e^{-\sqrt{\frac{2}{3}}\frac{\phi}{M_{\mathrm{P}}}} h^2 (gW_\mu^3 - g'B_\mu)(gW_\nu^3 - g'B_\nu) \Bigg]$$

$$- g_{E\mu\nu} \left(\frac{1}{2} G_{IJ} g_E^{\alpha\beta} D_\alpha \phi^I D_\beta \phi^J + V_0(\phi^I) + \frac{2M_{\mathrm{P}}^2}{\xi_R \Lambda^2 \sqrt{-g_E}} F(\phi^I) e^{\sqrt{\frac{2}{3}}\frac{\phi}{M_{\mathrm{P}}}} B_{\alpha\beta} \tilde{B}^{\alpha\beta} \right.$$

$$+ \frac{1}{4} g_E^{\alpha\rho} g_E^{\beta\sigma} B_{\alpha\beta} B_{\rho\sigma} + \frac{1}{4} g_E^{\alpha\rho} g_E^{\beta\sigma} W_{\alpha\beta}^i W_{\rho\sigma}^i + \frac{1}{4} e^{-\sqrt{\frac{2}{3}}\frac{\phi}{M_{\mathrm{P}}}} g_E^{\alpha\beta} g^2 h^2 \frac{(W_\alpha^1 - iW_\alpha^2)}{\sqrt{2}} \frac{(W_\beta^1 + iW_\beta^2)}{\sqrt{2}}$$

$$\left. + \frac{1}{8} e^{-\sqrt{\frac{2}{3}}\frac{\phi}{M_{\mathrm{P}}}} g_E^{\alpha\beta} h^2 (gW_\alpha^3 - g'B_\alpha)(gW_\beta^3 - g'B_\beta) \right) + e^{-\sqrt{\frac{2}{3}}\frac{\phi}{M_{\mathrm{P}}}} \bar{f} e_\mu^a \tilde{\gamma}_a \nabla_\nu^f f. \tag{C5}$$

APPENDIX D: THE VALLEY APPROXIMATION

In this section, we detail aspects of the so-called valley approximation for V_0. In this approximation, the system essentially behaves as a single-field scenario. First, for positivity of the potential at the inflationary scale, one requires

$$\lambda + \frac{\xi_H^2}{4\xi_R} > 0. \tag{D1}$$

For solving the background equations and the inflationary dynamics we focus on the R^2-like regime and the initial condition of the valley approximation derives from

$$\frac{\partial V_0}{\partial h} = 0, \tag{D2}$$

which gives three solutions

$$h = 0, \quad \text{and} \quad h = \pm \frac{\sqrt{e^{\sqrt{\frac{2}{3}}\frac{\phi}{M_{\mathrm{P}}}} - 1}}{\sqrt{4\lambda + \frac{\xi_H^2}{\xi_R}}} \sqrt{\frac{\xi_H}{\xi_R}} M_{\mathrm{P}}. \tag{D3}$$

One may choose the trivial solution $h = 0$, or the solution with a positive sign for convenience.

APPENDIX E: NUMERICAL SOLUTIONS OF THE ELECTROMAGNETIC EQUATIONS

In the following, we summarize the details of solving the mode equation of Eq. (4.15) in cosmological time t using the RK4 method

$$\ddot{u}^\lambda + H\dot{u}^\lambda + \left(\frac{k^2}{a^2} + \frac{8\cos^2\theta_W M_{\mathrm{P}}^2}{\xi_R \Lambda^2 a} \partial_0 (F(\varphi^I) e^{\sqrt{\frac{2}{3}}\varphi/M_{\mathrm{P}}}) \lambda k \right) u^\lambda$$
$$= 0. \tag{E1}$$

First, as required for the RK4 method, we rewrite the above equation as two first order equations

$$\frac{du^\lambda}{dt} = y^\lambda$$

$$\text{and,} \quad \frac{dy^\lambda}{dt} = -y^\lambda H - \left(\frac{k^2}{a^2} + \frac{8\cos^2\theta_W M_{\mathrm{P}}^2}{\xi_R \Lambda^2 a} \right.$$
$$\left. \times \partial_0 (F(\varphi^I) e^{\sqrt{\frac{2}{3}}\varphi/M_{\mathrm{P}}}) \lambda k \right) u^\lambda \tag{E2}$$

The equations are essentially in the form of

$$\frac{du^\lambda}{dt} = f(u^\lambda, y^\lambda, t), \quad \text{and} \quad \frac{dy^\lambda}{dt} = g(u^\lambda, y^\lambda, t), \tag{E3}$$

with

$$f(u^\lambda, y^\lambda, t) = y^\lambda,$$

$$g(u^\lambda, y^\lambda, t) = -y^\lambda H - \left(\frac{k^2}{a^2} + \frac{8\cos^2\theta_W M_{\mathrm{P}}^2}{\xi_R \Lambda^2 a} \right.$$
$$\left. \times \partial_0 (F(\varphi^I) e^{\sqrt{\frac{2}{3}}\varphi/M_{\mathrm{P}}}) \lambda k \right) u^\lambda. \tag{E4}$$

Now the task is to find out u^λ and y for each time step utilizing the RK4 method. This is provided by

$$u_{i+1}^\lambda = u_i^\lambda + \frac{1}{6}(l_0 + 2l_1 + 2l_2 + l_3),$$

$$y_{i+1}^\lambda = y_i^\lambda + \frac{1}{6}(m_0 + 2m_1 + 2m_2 + m_3), \tag{E5}$$

with

$$l_0 = \delta t\, f(u_i^\lambda, y_i^\lambda, t_i),$$

$$m_0 = \delta t\, g(u_i^\lambda, y_i^\lambda, t_i),$$

$$l_1 = \delta t\, f\left(u_i^\lambda + \frac{1}{2}l_0, y_i^\lambda + \frac{1}{2}m_0, t_i + \frac{1}{2}\delta t \right),$$

$$m_1 = \delta t\, g\left(u_i^\lambda + \frac{1}{2}l_0, y_i^\lambda + \frac{1}{2}m_0, t_i + \frac{1}{2}\delta t \right),$$

$$l_2 = \delta t\, f\left(u_i^\lambda + \frac{1}{2}l_1, y_i^\lambda + \frac{1}{2}m_1, t_i + \frac{1}{2}\delta t \right),$$

$$m_2 = \delta t\, g\left(u_i^\lambda + \frac{1}{2}l_1, y_i^\lambda + \frac{1}{2}m_1, t_i + \frac{1}{2}\delta t \right),$$

$$l_3 = \delta t\, f(u_i^\lambda + l_2, y_i + m_2, t_i),$$

$$m_3 = \delta t\, g(u_i^\lambda + l_2, y_i + m_3, t_i), \tag{E6}$$

where δt is the time step. The Bunch-Davis initial conditions for the modes u^λ and y are given in Eq. (4.19).

One can in principle fix the number of modes N_k in each time step within $[k_{\min}, k_c]$ for the integration of Eqs. (4.16). However, this makes the initialization of the modes in the next time step more involved. This is because as k_c increases in each time step, keeping N_k fixed each time would require some more involved initialization for subsequent time steps. We can take a simpler route and keep the number of k modes the same for all time steps. This ensures that the number of modes N_k and the corresponding modes are identical at each time step. In practice, we take a large range $[k_{\min}, k_{\max}]$ with $k_{\max} = Ca(t_{\mathrm{numend}})H(t_{\mathrm{numend}})$ where t_{numend} is the numerical end of our simulation. We chose $C = 100$ to ensure that $k_c(t_{\mathrm{numend}}) < k_{\max}$ and divide the range $[k_{\min}, k_{\max}]$ into $N_k = 200$ intervals. In each time step, we then numerically interpolate Eqs. (4.16) in $[k_{\min}, k_{\max}]$ and truncate the numerical integration up to the corresponding k_c values. Increasing N_k to higher values does not significantly impact our results. For further details of the numerical procedure, we refer the reader to Ref. [65].

In the presence of the Schwinger effect the corresponding equation of motion, Eq. (4.30), is solved numerically using similar methods as those described above.

[1] A. A. Starobinsky, Phys. Lett. **91B**, 99 (1980).
[2] K. Sato, Mon. Not. R. Astron. Soc. **195**, 467 (1981).
[3] A. H. Guth, Phys. Rev. D **23**, 347 (1981).
[4] Y. Akrami *et al.* (Planck Collaboration), Astron. Astrophys. **641**, A10 (2020).
[5] A. A. Starobinsky, Sov. Astron. Lett. **9**, 302 (1983).
[6] A. Vilenkin, Phys. Rev. D **32**, 2511 (1985).
[7] M. B. Mijic, M. S. Morris, and W.-M. Suen, Phys. Rev. D **34**, 2934 (1986).
[8] K.-i. Maeda, Phys. Rev. D **37**, 858 (1988).
[9] G. Aad *et al.* (ATLAS Collaboration), Phys. Lett. B **716**, 1 (2012).
[10] S. Chatrchyan *et al.* (CMS Collaboration), Phys. Lett. B **716**, 30 (2012).
[11] F. L. Bezrukov and M. Shaposhnikov, Phys. Lett. B **659**, 703 (2008).
[12] A. O. Barvinsky, A. Y. Kamenshchik, and A. A. Starobinsky, J. Cosmol. Astropart. Phys. 11 (2008) 021.

[13] F. Bezrukov, A. Magnin, M. Shaposhnikov, and S. Sibiryakov, J. High Energy Phys. 01 (2011) 016.

[14] F. Bezrukov, Classical Quantum Gravity **30**, 214001 (2013).

[15] A. De Simone, M. P. Hertzberg, and F. Wilczek, Phys. Lett. B **678**, 1 (2009).

[16] F. L. Bezrukov, A. Magnin, and M. Shaposhnikov, Phys. Lett. B **675**, 88 (2009).

[17] A. O. Barvinsky, A. Y. Kamenshchik, C. Kiefer, A. A. Starobinsky, and C. F. Steinwachs, Eur. Phys. J. C **72**, 2219 (2012).

[18] B. L. Spokoiny, Phys. Lett. **147B**, 39 (1984).

[19] T. Futamase and K.-i. Maeda, Phys. Rev. D **39**, 399 (1989).

[20] D. S. Salopek, J. R. Bond, and J. M. Bardeen, Phys. Rev. D **40**, 1753 (1989).

[21] R. Fakir and W. G. Unruh, Phys. Rev. D **41**, 1783 (1990).

[22] L. Amendola, M. Litterio, and F. Occhionero, Int. J. Mod. Phys. A **05**, 3861 (1990).

[23] D. I. Kaiser, Phys. Rev. D **52**, 4295 (1995).

[24] J. L. Cervantes-Cota and H. Dehnen, Nucl. Phys. **B442**, 391 (1995).

[25] E. Komatsu and T. Futamase, Phys. Rev. D **59**, 064029 (1999).

[26] C. P. Burgess, H. M. Lee, and M. Trott, J. High Energy Phys. 09 (2009) 103.

[27] J. L. F. Barbon and J. R. Espinosa, Phys. Rev. D **79**, 081302 (2009).

[28] C. P. Burgess, H. M. Lee, and M. Trott, J. High Energy Phys. 07 (2010) 007.

[29] M. P. Hertzberg, J. High Energy Phys. 11 (2010) 023.

[30] I. Antoniadis, A. Guillen, and K. Tamvakis, J. High Energy Phys. 08 (2021) 018; 05 (2022) 074(E).

[31] M. P. DeCross, D. I. Kaiser, A. Prabhu, C. Prescod-Weinstein, and E. I. Sfakianakis, Phys. Rev. D **97**, 023526 (2018).

[32] Y. Ema, R. Jinno, K. Mukaida, and K. Nakayama, J. Cosmol. Astropart. Phys. 02 (2017) 045.

[33] E. I. Sfakianakis and J. van de Vis, Phys. Rev. D **99**, 083519 (2019).

[34] Y. Ema, Phys. Lett. B **770**, 403 (2017).

[35] A. Salvio and A. Mazumdar, Phys. Lett. B **750**, 194 (2015).

[36] S. Pi, Y.-l. Zhang, Q.-G. Huang, and M. Sasaki, J. Cosmol. Astropart. Phys. 05 (2018) 042.

[37] D. Gorbunov and A. Tokareva, Phys. Lett. B **788**, 37 (2019).

[38] A. Gundhi and C. F. Steinwachs, Nucl. Phys. **B954**, 114989 (2020).

[39] M. He, A. A. Starobinsky, and J. Yokoyama, J. Cosmol. Astropart. Phys. 05 (2018) 064.

[40] M. He, R. Jinno, K. Kamada, S. C. Park, A. A. Starobinsky, and J. Yokoyama, Phys. Lett. B **791**, 36 (2019).

[41] D. Y. Cheong, S. M. Lee, and S. C. Park, J. Cosmol. Astropart. Phys. 01 (2021) 032.

[42] F. Bezrukov, D. Gorbunov, C. Shepherd, and A. Tokareva, Phys. Lett. B **795**, 657 (2019).

[43] M. He, R. Jinno, K. Kamada, A. A. Starobinsky, and J. Yokoyama, J. Cosmol. Astropart. Phys. 01 (2021) 066.

[44] F. Bezrukov and C. Shepherd, J. Cosmol. Astropart. Phys. 12 (2020) 028.

[45] M. He, J. Cosmol. Astropart. Phys. 05 (2021) 021.

[46] S. Aoki, H. M. Lee, A. G. Menkara, and K. Yamashita, J. High Energy Phys. 05 (2022) 121.

[47] G. R. Farrar and M. E. Shaposhnikov, Phys. Rev. Lett. **70**, 2833 (1993); **71**, 210(E) (1993).

[48] G. R. Farrar and M. E. Shaposhnikov, Phys. Rev. D **50**, 774 (1994).

[49] M. B. Gavela, P. Hernandez, J. Orloff, and O. Pene, Mod. Phys. Lett. A **9**, 795 (1994).

[50] K. Kajantie, M. Laine, K. Rummukainen, and M. E. Shaposhnikov, Nucl. Phys. **B493**, 413 (1997).

[51] A. D. Sakharov, Pis'ma Zh. Eksp. Teor. Fiz. **5**, 32 (1967).

[52] M. E. Shaposhnikov, Nucl. Phys. **B287**, 757 (1987).

[53] K. Kamada and A. J. Long, Phys. Rev. D **94**, 063501 (2016).

[54] M. M. Anber and L. Sorbo, J. Cosmol. Astropart. Phys. 10 (2006) 018.

[55] K. Bamba, Phys. Rev. D **74**, 123504 (2006).

[56] K. Bamba, C. Q. Geng, and S. H. Ho, Phys. Lett. B **664**, 154 (2008).

[57] M. M. Anber and L. Sorbo, Phys. Rev. D **81**, 043534 (2010).

[58] M. M. Anber and E. Sabancilar, Phys. Rev. D **92**, 101501 (2015).

[59] Y. Cado and E. Sabancilar, J. Cosmol. Astropart. Phys. 04 (2017) 047.

[60] K. Kamada and A. J. Long, Phys. Rev. D **94**, 123509 (2016).

[61] D. Jiménez, K. Kamada, K. Schmitz, and X.-J. Xu, J. Cosmol. Astropart. Phys. 12 (2017) 011.

[62] V. Domcke, B. von Harling, E. Morgante, and K. Mukaida, J. Cosmol. Astropart. Phys. 10 (2019) 032.

[63] Y. Cado, B. von Harling, E. Massó, and M. Quirós, J. Cosmol. Astropart. Phys. 07 (2021) 049.

[64] Y. Cado and M. Quirós, Phys. Rev. D **106**, 055018 (2022).

[65] Y. Cado and M. Quirós, Phys. Rev. D **106**, 123527 (2022).

[66] R. Durrer, O. Sobol, and S. Vilchinskii, Phys. Rev. D **106**, 123520 (2022).

[67] R. Durrer, O. Sobol, and S. Vilchinskii, Phys. Rev. D **108**, 043540 (2023).

[68] O. Savchenko and Y. Shtanov, J. Cosmol. Astropart. Phys. 10 (2018) 040.

[69] K. Subramanian, Rep. Prog. Phys. **79**, 076901 (2016).

[70] R. Durrer and A. Neronov, Astron. Astrophys. Rev. **21**, 62 (2013).

[71] V. Domcke and K. Mukaida, J. Cosmol. Astropart. Phys. 11 (2018) 020.

[72] H. Kitamoto and M. Yamada, J. High Energy Phys. 06 (2022) 103.

[73] T. D. Cohen and D. A. McGady, Phys. Rev. D **78**, 036008 (2008).

[74] Y. Cado and M. Quirós, Phys. Rev. D **108**, 023508 (2023).

[75] J.-O. Gong and T. Tanaka, J. Cosmol. Astropart. Phys. 03 (2011) 015; 02 (2012) E01.

[76] D. I. Kaiser, E. A. Mazenc, and E. I. Sfakianakis, Phys. Rev. D **87**, 064004 (2013).

[77] M. Sasaki and E. D. Stewart, Prog. Theor. Phys. **95**, 71 (1996).

[78] C. Gordon, D. Wands, B. A. Bassett, and R. Maartens, Phys. Rev. D **63**, 023506 (2000).

[79] S. Groot Nibbelink and B. J. W. van Tent, arXiv:hep-ph/0011325.

[80] S. Groot Nibbelink and B. J. W. van Tent, Classical Quantum Gravity **19**, 613 (2002).

[81] D. Wands, N. Bartolo, S. Matarrese, and A. Riotto, Phys. Rev. D **66**, 043520 (2002).

[82] D. Seery and J. E. Lidsey, J. Cosmol. Astropart. Phys. 09 (2005) 011.

[83] C. M. Peterson and M. Tegmark, Phys. Rev. D **83**, 023522 (2011).

[84] C. M. Peterson and M. Tegmark, Phys. Rev. D **87**, 103507 (2013).

[85] J. Elliston, D. Seery, and R. Tavakol, J. Cosmol. Astropart. Phys. 11 (2012) 060.

[86] M. P. DeCross, D. I. Kaiser, A. Prabhu, C. Prescod-Weinstein, and E. I. Sfakianakis, Phys. Rev. D **97**, 023527 (2018).

[87] M. P. DeCross, D. I. Kaiser, A. Prabhu, C. Prescod-Weinstein, and E. I. Sfakianakis, Phys. Rev. D **97**, 023528 (2018).

[88] S. M. Lee, T. Modak, K.-y. Oda, and T. Takahashi, Eur. Phys. J. C **82**, 18 (2022).

[89] H. Kodama and M. Sasaki, Prog. Theor. Phys. Suppl. **78**, 1 (1984).

[90] V. F. Mukhanov, H. A. Feldman, and R. H. Brandenberger, Phys. Rep. **215**, 203 (1992).

[91] K. A. Malik and D. Wands, Phys. Rep. **475**, 1 (2009).

[92] M. Sasaki, Prog. Theor. Phys. **76**, 1036 (1986).

[93] V. F. Mukhanov, Sov. Phys. JETP **67**, 1297 (1988).

[94] R. Easther and J. T. Giblin, Phys. Rev. D **72**, 103505 (2005).

[95] D. Langlois and S. Renaux-Petel, J. Cosmol. Astropart. Phys. 04 (2008) 017.

[96] C. M. Peterson and M. Tegmark, Phys. Rev. D **84**, 023520 (2011).

[97] B. A. Bassett, S. Tsujikawa, and D. Wands, Rev. Mod. Phys. **78**, 537 (2006).

[98] K. D. Lozanov and M. A. Amin, J. Cosmol. Astropart. Phys. 06 (2016) 032.

[99] E. V. Gorbar, K. Schmitz, O. O. Sobol, and S. I. Vilchinskii, Phys. Rev. D **104**, 123504 (2021).

[100] J. R. C. Cuissa and D. G. Figueroa, J. Cosmol. Astropart. Phys. 06 (2019) 002.

[101] M. D'Onofrio and K. Rummukainen, Phys. Rev. D **93**, 025003 (2016).

[102] M. D'Onofrio, K. Rummukainen, and A. Tranberg, Phys. Rev. Lett. **113**, 141602 (2014).

[103] M. Joyce and M. E. Shaposhnikov, Phys. Rev. Lett. **79**, 1193 (1997).

[104] B. A. Bassett, C. Gordon, R. Maartens, and D. I. Kaiser, Phys. Rev. D **61**, 061302 (2000).

[105] A. R. Liddle, D. H. Lyth, K. A. Malik, and D. Wands, Phys. Rev. D **61**, 103509 (2000).

[106] N. Barnaby and M. Peloso, Phys. Rev. Lett. **106**, 181301 (2011).

[107] N. Barnaby, E. Pajer, and M. Peloso, Phys. Rev. D **85**, 023525 (2012).

[108] T. Modak, L. Röver, B. M. Schäfer, B. Schosser, and T. Plehn, SciPost Phys. **15**, 047 (2023).

[109] S. M. Lee, T. Modak, K.-y. Oda, and T. Takahashi, J. Cosmol. Astropart. Phys. 08 (2023) 045.

[110] P. Collas and D. Klein, *The Dirac Equation in Curved Spacetime: A Guide for Calculations*, Springer-Briefs in Physics (Springer, New York, 2019).